Laser Assisted Fabrication of rPI/ionic liquid/rPI Supercapacitors for Energy Storage Application

Hinna Jamil

Fall 2015 MS-Physics

Supervised by:

Dr. Syed Rizwan Hussain

(Associate Professor)

DEPARTMENT OF PHYSICS, SCHOOL OF NATURAL SCIENCES (SNS), NATIONAL UNIVERSITY OF SCIENCES & TECHNOLOGY (NUST) ISLAMABAD, PAKISTAN

National University of Sciences & Technology

MS THESIS WORK

We hereby recommend that the dissertation prepared under our supervision by: MS. HINNA JAMIL, Regn No. 00000117112 Titled: Laser assisted fabrication of rPI/Ionic Liquid/rPI Supercapacitor for Energy Storage Application be accepted in partial fulfillment of the requirements for the award of **MS** degree.

Examination Committee Members

1. Name: DR. MOHAMMAD ALI MOHAMMAD   Signature: _____

2. Name: DR. MUDASSIR IQBAL   Signature: _____

External Examiner: DR. JAVED SAGGU   Signature: _____

Supervisor's Name DR. SYED RIZWAN HUSSAIN   Signature: _____

_____
Head of Department

01-03-2019
_____
Date

COUNTERSINGED

Date: 01-03-2019

_____
Dean/Principal

THESIS ACCEPTANCE CERTIFICATE

Certified that final copy of MS thesis written by **Ms. Hinna Jamil** (Registration No. **00000117112**), of **School of Natural Sciences** has been vetted by undersigned, found complete in all respects as per NUST statutes/regulations, is free of plagiarism, errors, and mistakes and is accepted as partial fulfillment for award of MS/M.Phil degree. It is further certified that necessary amendments as pointed out by GEC members and external examiner of the scholar have also been incorporated in the said thesis.

Signature: _____

Name of Supervisor: Dr. Syed Rizwan Hussain

Date: _____01-03-2019_____

Signature (HoD): _____

Date: _____01-03-2019_____

Signature (Dean/Principal): _____

Date: _____01-03-2019_____

Dedicated

To

My beloved Parents

Acknowledgement

I am grateful to almighty **Allah** who helped and guided me in every step of my work and ease all the difficulties and blessed me with people who encouraged and guided me.

I would like to pay my special gratitude to my supervisor **Dr. Syed Rizwan** Hussain whose endless support and encouragement helped me to complete my research work.

I am grateful to the principal of the School of Natural Sciences **Prof. Dr. Habib Nasir** and Head of the Department of Physics **Dr. Shahid Iqbal**, for their help and support throughout the program. I would also like to thank my GEC members **Dr. Muddasir Iqbal** and **Dr. Mohammad Ali Mohammad** for their dedication and valuable suggestions to improve and enhance my research work.

I acknowledge support of my parents my husband and all my group fellows Ms Tayyaba Malik, Shayan Naveed, Ayesha Tariq, Mamoon Asghar, Zarah Khan and Momina Ahmed.

Contents

TABLE OF FIGURES

ABSTRACT

The increasing demand of the modern portable, scalable and wearable energy storage devices pushed the researchers to develop flexible, inexpensive and more efficient energy storage devices which possess high power and energy density. Supercapacitors and batteries has attracted great attention because of their high energy density, high power density and long-life cycle, but supercapacitors have edge over batteries due to their high-power density and long lifetime. Supercapacitors are widely used in hybrid vehicles, electronic devices and solar arrays etc. in this work a supercapacitor was fabricated by using a simple and cheap laser scribing technique. Polyimide (PI) sheet was used as a substrate and laser scribing method was used to change its structure and properties upon laser irradiations into a graphene like carbonaceous structure. Laser scribing have been widely used in printed electronics and we can also draw complex geometries and patterns with this facile technology. Supercapacitors were fabricated by pattering a 1x1cm electrode on the PI sheet by using laser of wavelength of 450nm. Two different ionic liquids ILs i.e. 1-methyl 3-octyl imidazolium bromide ([C8mim] Br) 1-methyl 3-butyl imidazolium bromide ([C4mim] Br) were tested as an electrolyte for laser scribed supercapacitors. The IL electrolytes were sandwiched between the reduced polyimide (rPI) electrodes. The maximum capacitance was calculated to be 3.8mF/cm2 for ([C8mim] Br) IL and 313µF/cm2 for ([C4mim] Br) IL at the scan rate of 20mV/s applying voltage window up to 2V. The galvanotactic charge discharge (CC) curves are of perfectly symmetric triangular curves showing good stability of the supercapacitor.

Chapter 1: Introduction

1.1. Flexible Electronics Devices

In recent years flexible electronics attracted so much attention in industries and academia. Flexible electronics are in lime light due to low manufacturing cost, light weight, simple fabrication, and accessibility of affordable flexible substrates e.g. papers, plastics and textiles. Flexible electronics have wide range of applications flexible display, flexible solar cell, optoelectronic (light-emitting or photovoltaic diodes), thin-film transistors (TFTs),printed RFID and flexible lighting etc.[1] Instead of bulky rigid substrate thin flexible substrates are used for flexible electronics. So, they are lighter, smaller and easy to use than rigid electronics. Flexible electronics are favorable for practical use, materials used in these devices are highly durable under bending. Different flexible conductors (i.e. metal nanowires, conducting polymers, carbon nanotubes, and graphene) for optoelectronics applications have been tested which have high tolerance, chemical stability and low-cost fabrication. Graphene found to be a most promising candidate because of its unique properties which are highly favorable in flexible electronics.[2]

1.2. Background Flexible Electronics devices

History of Flexible electronics is old. The biggest motivation for flexible electronics was solar industry. energy crisis forced researcher s to work on thin films to reduce the cost of electricity. In early 80's organic polymer films aka plastic was used as a substrate for amorphous silicon solar cells. This was the first time that official study is carried out on the flexibility of solar cells.[3] Flexible can mean some distinct features i.e. bendable, well fitted shape, elastic, light, non-breakable, roll-to-roll processable, or large-area. It is a vast field with open boundaries which are further being pushed with its new development methods and application. Today industrial community for flexible electronics focuses more on flexible displays and sensors arrays for X-rays. Flexibility for researchers means well fitted displays and sensors, electronic textiles, and electronic skin. [4] The first flexible thin-film transistor (TFT) was made back in

1968, when TFT of tellurium was made on a paper strip by Brody and colleagues and they presented TFT matrices for display purpose. Brody's group used variety of substrate to make TFTs in the following years including Mylar sheets, polyethylene, and anodized aluminum wrapping foil. TFTs are so flexible that they can be bend up to a radius 1/16'' and continued to function. When cut in half along the channel direction their both halves are remained operational.[5, 6]

Polycrystalline silicon (poly-Si) TFTs fabricated on plastic substrate in 1997, using laser-annealing. Flexible electronics had been researched widely after that and different companies and research groups fabricated flexible displays even on steel or plastic foil substrate.[4]

1.3. Material for Flexible Electronics

Common large area electronic structures consist of (i) a substrate, (ii) backplane electronics, (iii) a front-plane, and (iv) encapsulation. For flexible structure all components should be able to bend up to some extent without losing their function. There are basic two procedures which have been practiced for making flexible electronics.

- Transfer of complete circuits to a flexible substrate.
- On flexible electrode a direct fabrication of circuits

Mostly the surface is covered with the electronics which is fabricated directly on the substrate, in many applications. Existing planar microfabrication techniques isn't compatible with commonly flexible substrates, so diverse ways are used to integrate various materials. Direct fabrication need to (i) depends on polycrystalline or amorphous semiconductors due to their fabrication on new substrates, (ii) to develop new techniques for processing, (iii) to introduce novel materials, and (iv) device performance should not be compromised by lowering of process temperatures tolerant substrates. In process research direct fabrication techniques on flexible materials as substreates is a seedbed. New techniques like etch masks printing, active device materials printing and electronic functions because of local chemical reaction.[7] Flexibility means various different properties which attract manufactures and users. These properties can be categorized in three different classes. Described in Fig. 1:

i. Bendable or rollable,
ii. Consistent in shape, and

iii.   Elastically stretchable.

Microfabrication tools have been polished and perfected for flat substrates. That is why today all fabrication is done on a smooth and uniform workpiece that is shaped only as delayed as possible in the process. The planar integrated circuits and display technology based on the benefits of this approach.
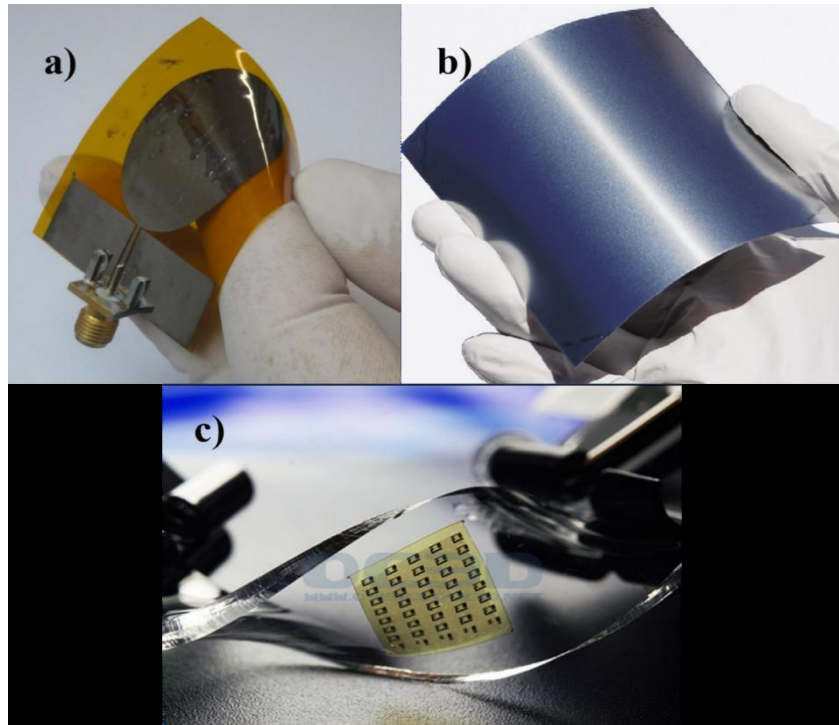
Figure 1   Three various kinds of flexible substrates: a) Polyimide (foldable and rollable), b) Stainless Steel (permanently deformed) and c) PDMS (elastically stretchable).

1.3.1. Flexible Substrates

There are three types of materials which can be used as a substrate for flexible device applications.

- Metals
- organic polymers and
- flexible glass.

1.3.1.1.Plastic Films

Polymer foils are very flexible, cheap and ideal for processing of devices on its roll. They are permeable to oxygen and water, also thermally they are less stable than glass substrate. However, polymers substrates have low coefficient of thermal expansion (CTE) and lack dimensional stability. Typically, polymer films shrink in size as they undergo various cycles of heating and cooling. The shrinking can be avoided if they are annealed for prolonged period.[8] Elastic modulus of polymer substrates is lower than that of the inorganic material devices, so during processing a small mismatch in CTE along with temperature may cause the breakage of device film. The ideal CTE for polymers is below 20ppm/^{o}C for silicon based device materials.[9]

Properties	PET	PEN	PC	PES	PI
	Melinex	Teonex	Lexan	Sumilite	Kapton
T_g, $\circ$C	78	121	150	223	410
CTE (–55 to 85$\circ$C), ppm/$\circ$C	15	13	60–70	54	30−60
Transmission (400–700 nm), %	89	87	90	90	Yellow
Moisture absorption, %	0.14	0.14	0.4	1.4	1.8
Young's modulus, Gpa	5.3	6.1	1.7	2.2	2.5
Tensile strength, Mpa	225	275	–	83	231
Density (gcm^{-3})	1.4	1.36	1.2	1.37	1.43
Refractive index	1.66	1.5–1.75	1.58	1.66	–
Birefringence, nm	46	–	14	13	–

Table 1. Potential candidates for plastic substrates.

For flexible substrates the potential polymers are (1) Semi-crystalline thermos plastic polymers e.g. polyethylene naphthalene (PEN) and polyethylene terephthalate (PET) (2) Non-crystalline thermoplastic polymers e.g. polycarbonate (PC) and polyethersulphone (PES), and finally (3) Materials having high glass transition temperature (T_g) i.e. polyarylates (PAR), poly-cyclic olefin (PCO), and polyimide (PI).[10] PCO, PES, PAR, and PC have a high Tg however their

CTEs are round about 50ppm /^{o} C or higher, but they have poor resistance to process chemicals. According to research done on PEN, PET and PI which have small CTEs i.e. 13, 15 and 16 ppm/^{o} C respectively. They also have relatively high resistance to chemical processes. PET and PEN are optically transparent, have low water absorbance (~0.14%) but they have low process temperature i.e. ~150 and ~200℃ respectively, even after prolonged annealing. On the contrary PI has increased level of Tg of 350℃ and it is yellow in color as a result of absorbing blue light. It absorbs moisture approximately up to 1.8%. In flexible plastic substrates the permeation rate for water is 1–10 g/m^2/day and for oxygen it is 1–10 cm^3/m^2/day which doesn't match with the requirement and i.e. 10^{-6} g/m^2/day and 10−5 cm^3/m^2/day for water and oxygen respectively.[11]

1.3.1.2.   POLYIMIDE (SUBSTRATE)

Polyimide is a well-known thermally stable polymer which is widely used as adhesives, films, dielectric, foams, plastic moldings, matrices of resin for composites and wire coating for enamels. Polyimides are a class of polymers which are heteroaromatic and highly resistant to heat.[12] Polyimide have variety of applications in defense, aerospace, fiber optics and opto-electronics.

Polyimide films are synthesized via solution casting method in which polyamic precursor solution is deposited on a substrate and after applying excessive heat more than 300° C it is converted into polyimide or it can be done through some chemical means. Another method for casting films is through phenolic solvents. A polyamic acid derived from the reaction ODA (4,4'-diaminodiphenylether) and BPDA (3,3',4,4'-biphenyltetracarboxylic dianhydride) known as ODA-BPDA. From its p-chlorophenol solvent, it is casted onto a supportive substrate, after that it is heated over 300° C for imidization and also to dried of the solvent. ODA precursor is used by Ube Industries as known as Upilex R. Similar procedures are used to cast commercially famous product such as Kapton®.[13]

1.4. Fabrication Techniques for Flexible Electronics

There are various micro and Nano-fabrication techniques which have been used to fabricate flexible electronics devices. The aim of these techniques is to fabricate a miniature structure of micro or nanoscale level. By miniaturization of structures is to lower their production cost, to increase the density of components and its performance per device and per integrated circuit.

Microfabrication techniques classified into following groups.

Property transformation: It include alteration of a substrate by doping or by ion implantation. Impurities are intentionally introduced during the process of doping while in ion implantation ion of some material is implanted into a substrate of another solid material.

Microfabrication via pattering: This technique is based on lithography i.e. Photolithography and soft lithography. In photolithography a geometric pattern is transferred by using light and a photomask on to a photoresist which is deposited on a substrate. On the other hand, in the case of soft lithography a certain structure in replicate using moulds, elastomeric stamps or photomasks.

Additive microfabrication: it involves condensation or growth of certain material layer on a substrate. e.g. (i) thermal oxidation, is used to produce a thin oxide layer on a wafer surface, (ii) chemical vapor deposition (CVD), a chemical process which is used to produce highly pure solid materials having improved performance. (iii) Physical vapor deposition (PVD) is microfabrication technique in which vaporized materials are condensed making a thin film on a surface. (iv) Epitaxy is method in which a monocrystalline film is deposited on a monocrystalline substrate.

Subtractive microfabrication: this technique employs patterning a microstructure by etching or removing a portion of a substrate. subtractive microfabrication technique is divided into two types (i) Dry etching, i.e. removal of a material by bombarding it with ions (e.g. plasma of reactive gases) that removes the exposed portion of the material surface. (ii) Wet etching, this chemical etching in which a chemical is used for etching instead of plasma.[14]

1.3.1 Laser Scribing

Laser scribing is also a microfabrication technique, this technique in only applicable on certain materials such as polyimide, graphene oxide, polyetherimide etc. in this technique laser irradiation change the composition and the morphology of material. When a polyimide film is exposed to the laser radiations a photothermal reduction takes place which causes the removal of certain functional groups from its surface making that area to be conductive. This is environment friendly and a cost-effective method with a minimum chemical loss. In direct laser writing we use a pre-polymer and then we polymerize it, but in laser scribing a thin film or a substrate is reduced by thermal irradiations. Thin films of reduced polyimide RPI and reduced graphene

oxide rGO produced from laser irradiations have much higher conductivity. This technique is a one-step synthesis, less time consuming, environment friendly and inexpensive.
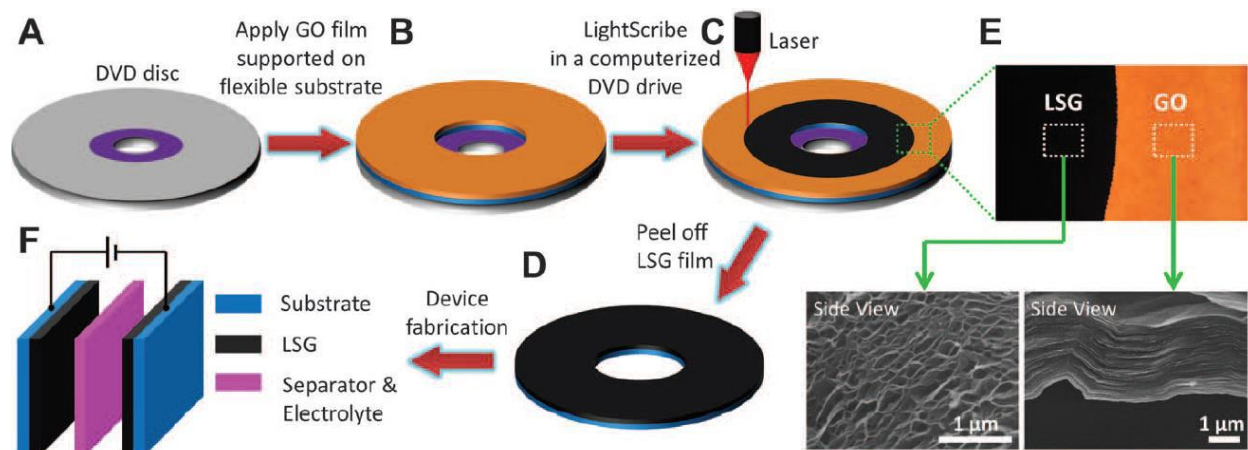
Figure 2 A process flow of laser scribing through a DVD burner. Copyright 2018 by The American Association for the Advancement of Science. Reprinted with permission.

1.5. Energy Storage Devices

The successful development of portable and wearable energy storage devices promotes the design of flexible energy storage systems.[15] It is very essential nowadays to develop novel, inexpensive and ecofriendly energy storage systems, according to the need of modern society and transpiring ecological concerns.[16] Flexible energy storage devices like supercapacitors and batteries attracted tremendous attention.[15] performance of energy storage devices can be enhanced by increasing their energy density and power density, so many efforts have been made to synthesize advanced and novel electrode materials with tailored structure, composition and morphology. The main aim of the researchers is devising the nanostructured active materials which are also highly conductive providing enormous potential to attain excellent energy storage, high rate capabilities and increased lifespan for electrode materials.[17]

Graphene is a monolayer of 2D sp^2 hybridized carbon atoms packed together to form honeycomb lattices. Graphene has attracted great interest in research because of its distinct structural features i.e. increased surface area, enhanced thermal and chemical constancy, increased conductivity and

mechanical strength and flexibility. All these unique properties make graphene favorable for energy storage applications. There are different derivatives of graphene e.g. Graphene oxide (GO) and reduced graphene oxide (RGO) from which we constructed more graphene based materials and which are favorable suitors to serve as electrodes for energy storage devices such as Lithium ion batteries (LIBs) and Supercapacitors (SCs).[15]

To produce graphene different techniques have been developed, i.e. mechanical exfoliation, chemical exfoliation, and chemical vapor deposition (CVD).

Mechanical exfoliation is easy and affordable procedure which create flawless graphene layers; nevertheless, large area graphene layers can't be achieved. Large sheets of graphene can be obtained from CVD; but this process is complicated and costly, because of its expensive processing equipment. Different attempts have been done to investigate diverse ways of fabricating inexpensive large area graphene. Graphene oxide from which graphene layers can be reduced are ideal suitors for devices like solar cells, supercapacitors and light emitting diodes(LEDs). Variety of techniques and procedure have been investigated to produce reduced graphene oxide (rGO). These methods arereduction of hydrazine hydrate, hydrogen plasma reduction, light reduction, and thermal reduction. The rGO produced from chemical reduction which is a scalable method, gives a poor yields of surface area and electrical conductivity. El-Kady et al. have used commercially available CD/DVD optical drive and converted graphene oxide (GO) into reduce graphene oxide (rGO).[18]

1.5.1. Supercapacitors

Supercapacitors (SCs) which are also called electrochemical capacitors are energy storage devices that can store and liberate energy at high charge discharge rate. They possess high power capability and large current density. They have long life cycle life i.e. up to 100 000 cycles and they also exhibit fast charge propagation. [5] Supercapacitors exhibit high Energy density i.e. several orders of magnitude than that of conventional capacitors. A supercapacitor comprised of two electrodes immersed in an electrolyte and separated by a porous membrane/separator.

Based on the charge storage mechanism there are three types of supercapacitors.
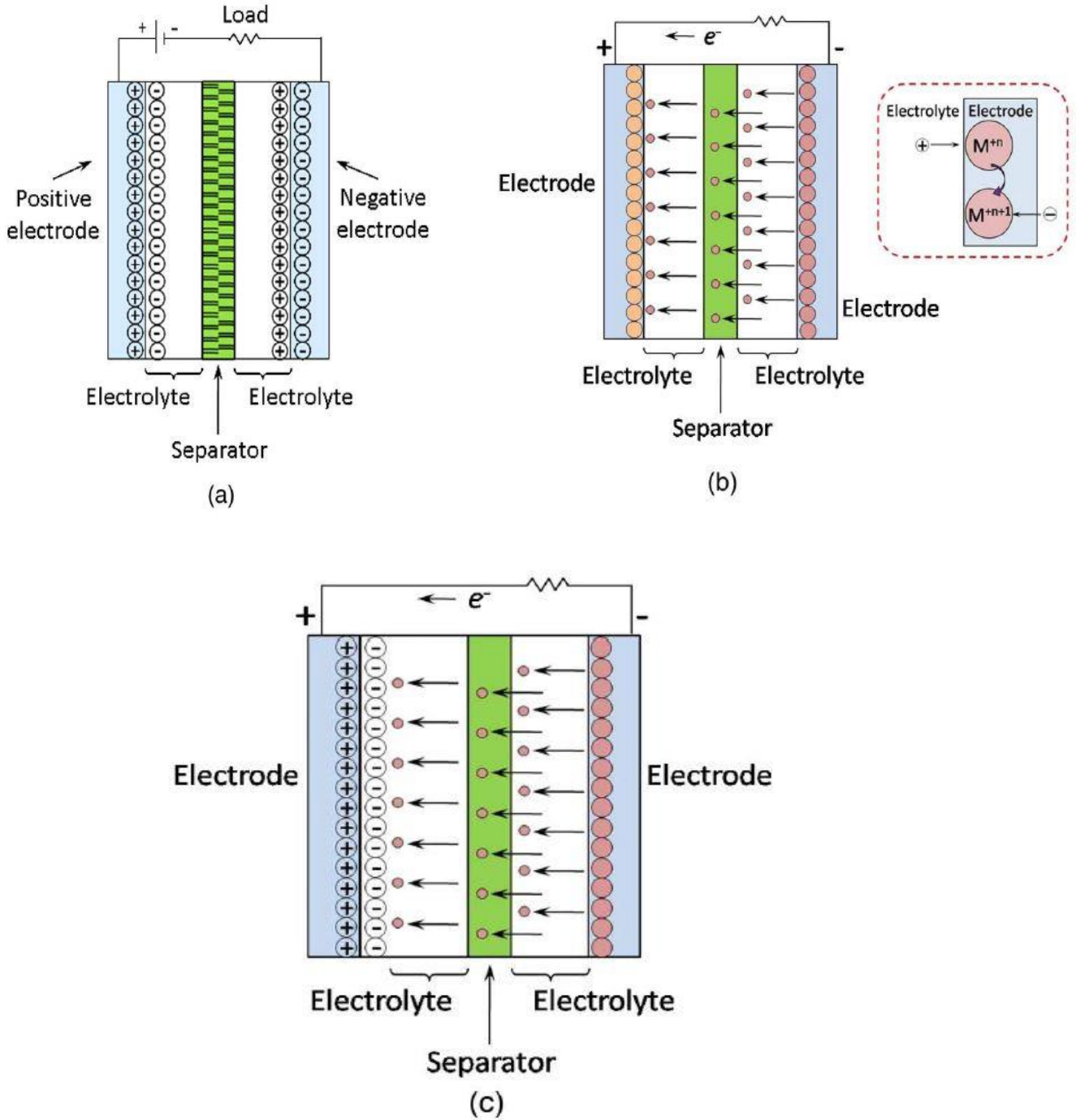
Figure 3 Schematic diagram types of supercapacitors: (a) EDLC type; (b) pseudo-capacitor type; (c) hybrid-capacitor. [19]
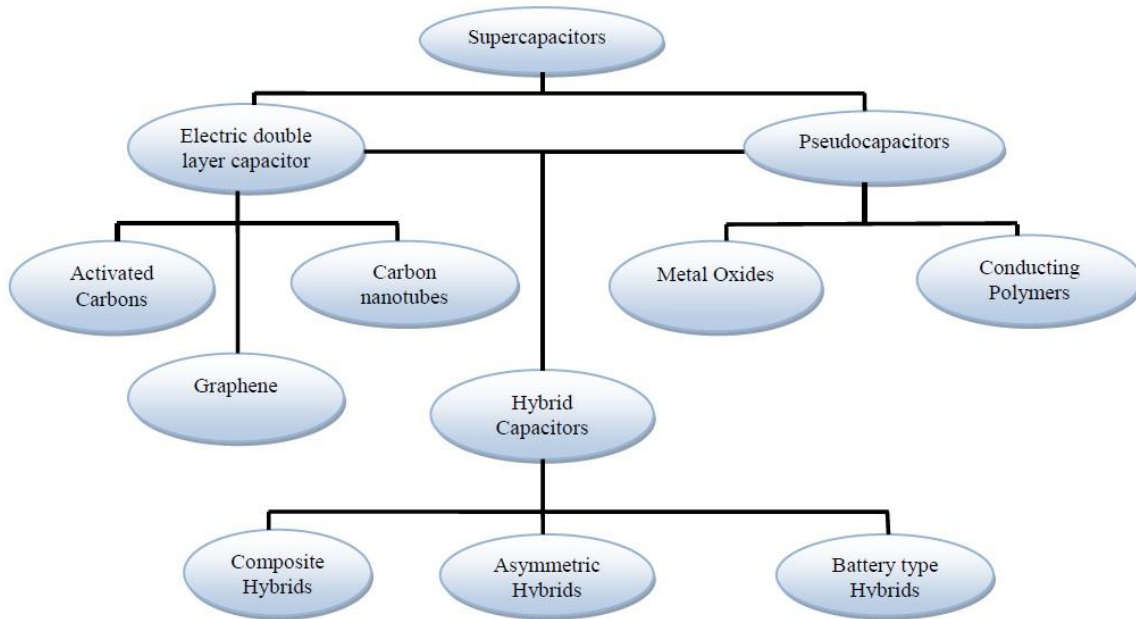
Figure 4 Taxonomy of supercapacitors

.

1.5.1.1.   Electrochemical double layer capacitors (EDLCs)

In electrochemical double layer capacitors (EDLCs) the electrode is typically made of activated carbon and an electrolyte is used between the electrodes isolated by a separator, and the charge storage mechanism is a pure electrostatic attraction or via non- faradic process which occurs between the ions that are accumulated at the interface of electrode and electrolyte. [6] The more accessible surface area and pore size distribution of electrode materials effect the storage capacity of an EDLC. Carbon materials having all these features and their easy accessibility, simple processing, and high chemical stability are more suitable candidate as an electrode material for EDLCs. [1] The energy is stored in an electrochemical double layer. Charge will have accumulated on the electrode surfaces as the voltage is applied. Attraction of opposite charges occur due to the potential difference and the ions in the electrolyte will start to diffuse onto the pores of oppositely charged electrodes and on the surface of separator. Recombination of the ions is avoided at the electrode because of the double layer. By increasing the specific surface area and decreasing the distances between the electrodes along with an electrochemical double layer a higher energy density can be attained in EDLCs.

The storage mechanism of EDLCs allows a very fast energy storage, delivery and high-power performance. In batteries during the charging and discharging swelling is observed in active materials, so this can be avoided in EDLCs as there is no chemical reaction because the process is non- faradic.

The difference between the EDLCs and Batteries

1. High cycle stability of EDLCs as compared to batteries which withstand only few thousands.
2. EDLCs are experiencing limited energy density as compared to batteries.

1.5.1.2.   Pseudo-capacitors

In pseudo-capacitors charge is stored via faradic process, electrons are transferred in Faradic reactions and reduction and oxidation is occurs on the electrode material e.g. using a conducting polymer. Charge storage mechanism in Pseudo-capacitors involves transfer of charge between electrode and electrolyte. The faradic current pass through the supercapacitor cell as the charge move across the double layer. In pseudo-capacitors due to faradic process higher specific capacitance and energy density is achieved as compare to EDLCs. As in pseudo-capacitors the oxidation reduction is involved just like batteries so they suffer with low cycle stability and power density. [6]

1.5.1.3.   Hybrid Capacitors

As EDLCs provide us with excellent cyclic stability and high-power output, while pseudo-capacitor offers greater specific capacitance hybrid capacitors offer both. This is achieved by joining energy source i.e. electrode of batteries and a power source of capacitor like electrode in one assembly. By selecting the correct electrode combination, it is possible to increase the cell voltage which in returns helps in improving the energy and power density. [7]

Comparison between Li ion batteries and SC

Supercapacitor is a device which behaves somewhere between a battery and a conventional capacitor. Charging and discharging of a supercapacitor is quick like a capacitor, but possesses 20–200 times incresed capacitance as compared to conventional capacitors. By comparing batteries with supercapacitors, SCs have higher power density but lower energy density. Energy is stored in batteries via redox reactions in the bulk electrode, which leads to high energy density but low power density due to slow kinetics. The higher rate capacity of super or ultra-capacitors

is due to the electrostatic storage mechanism, in which the charge is stored at the exterior of electrode. The Ion transportation is instant in the solution towards the electrode surface, which leads to fast charge and discharge capability. On the other hand, in batteries, electrons don't transfer at the interface. Charging and discharging of supercapacitors is very dynamic and there is no damage to the cell during this process and so they are ideal for power system applications and in hybrid vehicles. SC possess high reversible charging and discharging cycles and there is no phase change of electrodes during the process resulting in increased life cycle as compared to batteries. [8]
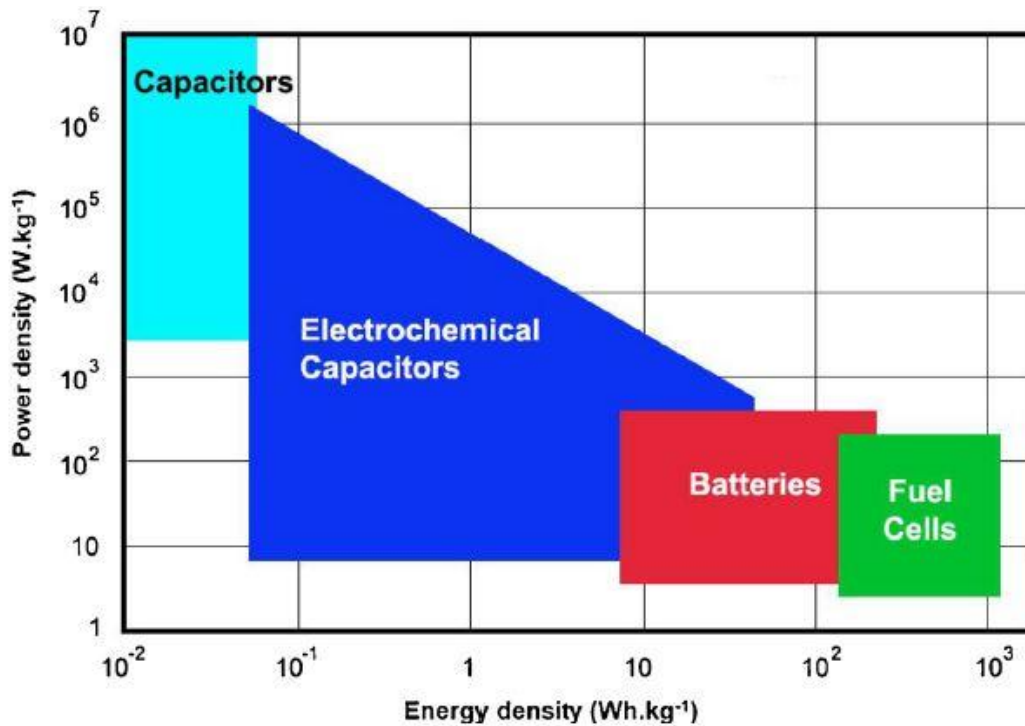
Figure 5 Ragone chart: graphical comparison between different energy storage devices, Power density as a function of energy density.

1.5.2. Applications

Supercapacitors are used in variety of applications where a large amount of energy can be store or release in a very small amount of time. Supercapacitors have been widely used in hybrid electric vehicles, electric vehicles and in fuel cell automobiles. SC can also be used in electronic devices like UPS and computers for memory backup. SC are used in micro energy harvesting applications i.e. solar arrays. They also have wide application in communications because of their capability to work at low temperatures and providing instant power.[20]

Chapter: 2 Literature Review

In recent few years energy storage devices such as Lithium ion batteries and supercapacitors have been focus of the research to meet the increasing demand of the more efficient energy storage devices. Main aim of the ongoing research is to develop new methods for cost effective environment friendly and more efficient miniaturized portable and flexible energy storage devices and still possess high power and energy densities.[21]

In recent investigation of research Carbon nanotubes (CNT) and graphene due to their excellent mechanical stability and great bending strength are ideal electrode material for bendable and stretchable electrochemical supercapacitors.[22]

Developing new techniques which are simple, inexpensive and don't require advanced processing to produce highly efficient micro-devices is very challenging. Unusual methods have been used for the production of graphene based micro-supercapacitors and these methods are so unique and have so much potential that it allows us easy, scalable and cost-effective fabrication.

Ajayan et al in 2011 developed an unconventional method for the fabrication of micro-supercapacitors via laser reduction and patterning of hydrated graphene oxide films. Using laser irradiations converting hydrated GO into RGO an active electrode. Reduction depth and resistivity of RGO depends upon laser power. A porous RGO electrode material was formed by laser heating, gives the highest specific capacitance of 0.51 mF cm^{-2} was determined from the in-plane circular design and the volumetric capacitance calculated to be 3.1 F cm^{-3}.[23]

Irradiation of infrared inside a standard LightScribe CD/DVD optical drive was used by El-Kady and co-workers in 2012 producing a laser scribed graphene (LSG) by reducing the Graphene oxide GO which was used as an electrochemical capacitors (ECs) electrode. A super thin device of thickness of 100 mm can be fabricated by using identical laser scribed electrodes and sandwiching a porous ion. The LSG will have surface area of 1520 m^{2}g^{-1} which is greater than the standard activated carbon material which helps increasing the capacity of charge storage which in returns results high volumetric and stacked capacitance. Laser irradiation exfoliate and reduce the GO sheets and produce an open LSG matrices network. Agglomeration of graphene sheets can be avoided by this method. The network like structure of RGO possess open pores

which facilitate the access of electrolyte to the surface of electrode. A thin flexible substrate of polyethylene terephthalate (PET) was used to assemble a uniform LSG-ECs and using H_3PO_4 as an electrolyte. The specific capacitance of the device was measured to be 3.67 mF/cm^2. Also, due to the leakage of the liquid electrolyte, it was replaced by polymer gel electrolyte (PVA-H_3PO_4). The porous structure of LSG electrode absorbed the gel electrolyte effectively resulting a high-performance device. LSG ECs was also examined by using an organic electrolyte. An organic electrolyte tetraethylammonium tetra fluoroborate was also examined which results in an enhanced performance having specific capacitance up to 4.82 mF/cm^2 along with wide operating voltage window of 3 volts. LSG ECs was also investigated using ionic liquid electrolyte i.e. 1-ethyl-3-methylimidazolium tetrafluoroborate (EMIMBF$_4$) which result in a high specific capacitance of 5.02 mF/cm^2. [24]

In 2014 Liu et al reduced Graphene oxide (GO) by using laser, flexible polyethylene terephthalate sheets were coated with the layers of GO/carbon nanotubes (CNTs)and then an integrated structure was patterned by laser converting it into laser scribed graphene (LSG)/CNTs micro-supercapacitors. Restacking of graphene sheets can be avoided b adding CNTs which also increase the ion accessible area significantly. Single walled (SW) CNTs and multi walled (MW) CNTs with different diameters were inserted between GO layers by using tip sonicating treatment resulting GO/CNTs hybrid powder. Polyethylene terephthalate (PET) pasted uniformly on the surface of DVD disc which is to be laser scribed and then the solutions of GO/CNTs were drop cast on the PET sheet and then dehydrated. Integrated structures were patterned on the GO/CNTs layers by using simple laser scribing DVD burner and a computer software. This integrated structure contains 8 positive and negative electrodes having width and interspacing of 150 μm and 5mm length. A solution of PVA/H_3PO_4 gel electrolyte was also prepared and drop cast on the laser scribed electrode. The volumetric capacitance of LSG-MSC is calculated to be 0.77 Fcm^{-3}, LSG/MWCNTs (60nm)-MSC having 1.2 Fcm^{-3}, LSG/MWCNTs (20nm)-MSC with 1.44 Fcm^{-3}, LSG/MWCNTs (8nm)-MSC with 1.65 Fcm^{-3}, and LSG/SWCNTs-MSC was calculated to be 2.20 Fcm^{-3}. These flexible solid-state supercapacitors exhibit excellent energy storage performance. This study shows that CNTs having less diameter increase the energy

storage performance of the MSC and highest volumetric capacitance i.e. 3.10 Fcm^{-3} is possessed by LSG/SWCNTS-MSC.[25]

M.H Amiri and coworkers in 2016 fabricated a supercapacitor having Graphene/ZnO nanocomposites as an electrode. A mixture of GO/ZnO was drop cast uniformly on a PET coated DVD disc and then dehydrate under ambient air. The GO/ZnO coated DVD drive was then set under DVD burner after laser irradiation a reduced graphene oxide rGO/ZnO composite was prepared with the mass ratio of 1:25 that of Zn $(NO_3)_2$. $6H_2O$ and GO. As a result, specific capacitance was increased at 0.1 mA/cm^2 of current density as compared to pure rGO electrodes. A uniform layer of KCL/PAAK gel electrolyte was spin coated on a laser scribed rGo/ZnO composite integrated electrode which shows the capacitance of 9 F/cm^3 at 150 mA/cm^2 of current density. The increased storage capacity per unit volume and power density of this micro supercapacitor was calculated to be 1.2 mWh/cm^3 and 70 mW/cm^3 respectively. The in plane ZnO/LSG flexible micro supercapacitor are also suitable at different bending angles.[26]

In 2015 Hwang et al demonstrated a simple synthesis and processing technique to form a LSG/Ruthenium oxide (RuO_2) nanocomposites electrodes. The homogenous mixture of GO and $RuCl_3$ hydrate was drop-cast on the surface of polyethylene terephthalate(PET) substrate which was pasted on a DVD disc. A commercial light scribe DVD burner is used to reduced graphene oxide and oxidized $RuCl_3$ to RuO_2. The nanoparticles of hydrous RuO_2 were attached successfully attached onto the surface of graphene. The RGO/ RuO_2 hybrid electrode using solution of H_2SO_4 as an electrolyte showed enhanced cyclic stability having specific capacitance up to 1139 F g^{-1} due to the fast electronic and ionic diffusion. These hybrid electrodes were also utilized aqueous symmetric asymmetric electrochemical supercapacitors resulting enhanced power density i.e. 12 kW/kg and low cost, resulting a hybrid electrochemical capacitor which is more efficient and excellent in performance. In plane hybrid micro supercapacitors can also be manufactured by using the same technique, and these micro-supercapacitors can also be integrated into components and connecting them into series or in parallel can increase the working potential and power of single cell. These devices are ideal for energy storage solutions because they have low internal resistance and excellent life cycle.[27]

A sandwich-type electrochemical energy storage device having potential window of 3 V was devised by H. Liu et al. in 2006. In this asymmetrical supercapacitor nickel-based mixed rare-

earth oxide (NMRO) was used as a mesoporous positive electrode and active carbon electrode which was treated with KOH was used as a negative electrode. A non-volatile, solvent free and water-resistant room temperature ionic liquid (RTIL) 1-butyl-3-methylimidazolium hexafluorophosphate (BMIM-PF$_6$) was coupled with these electrodes resulting in a significantly high energy density and power density of 50 Wh/kg and 458 W/kg respectively. No capacitance loss was found even after 500 cycles. The improved performance of electrodes is due to its more porous surface and formation of homogeneous granules. RTIL BMIM-PF$_6$ provides bulky conductive ions and wide electrochemical window and also continual wetting of active material electrode and separator which increased the durability of the supercapapcitor.[28]

In 2007 A. Balducci et al. fabricated a supercapacitor cell in which microporous activated carbon used as an active material for electrode and as an ionic liquid electrolyte i.e. N-butyl-N-methylpyrrolidinium bis(trifluoromethanesulfonyl)imide (PYR$_{14}$TFSI) was used. The electrochemical study was done by using threeelectrode cell assembly and specific capacitance was calculated to be 60 F/g at the scan rate of 20 mV/s. the maximum operating potential was attained to 4.5 V at 60° C. A double layer activated carbon supercapacitor having a coin cell AC/ PYR$_{14}$TFSI/AC assembly at 60° C and at working potential of 3.5 V was studied. It showed excellent cyclic stability the maximum specific energy was calculated to be 31 Wh/kg and maximum power density was measured to be 8.6 kW/kg. these supercapacitors are suitable for high temperature applications.[29]

T.Y Kim and C.W Bielawski et al in 2010 reported a high-performance poly ionic liquid (PIL) RGO electrode and ionic IL (1-ethyl-3-methylimidazolium bis(trifluoromethylsulfonyl) Amide) [EMIM-NTf$_2$] electrolyte based supercapacitor. The PIL: RGO materials are very much suitable for supercapacitors, and compatible for IL electrolytes because the provide IL ions access to graphene electrodes. The supercapacitor formed using PIL: RG-O as an electrode and EMIM-NTf$_2$ as an electrolyte shows stable electrochemical performance having high specific capacitance up to 187 Fg^{-1} which is due to the enhanced wettability of IL electrolyte on the PIL: RGO electrode material which results increased the surface area of the electrode enhancing the charge storage at electrode electrolyte interface. [30]

In 2009 A. Lewandowski et al. studied the properties of supercapacitor having activated carbon cloth (ACC) as an electrode they studied three different type of electrolytes i.e. aqueous, organic

and ionic liquids. N-methyl-N-propylpyrrolidinium bis(trifluoromethanesulfonyl)imide (MPPyrNTf$_2$) ionic liquid with its solution in molecular liquid acetonitrile (AN) and propylene carbonate (PC) at room temperature (25° C) was investigated. The supercapapcitor in which MPPyrNTf$_2$ was used as an electrolyte can work at the potential difference up to 3.5 V.posses the specific energy up to 200 kJ/kg which is higher than of all other electrolytes studied.[31]

Yao Chen and coworkers in 2010 reduced GO partially using hydrobromic acid HBr and fabricated it as an electrode for supercapacitor. HBr is weak reductant acid. This RGO electrode possessed some additional pseudo capacitance because there was some residue of oxygen functional groups present in that RGO. A capacitance of 158 F/g was obtained by using ionic liquid electrolyte 1-butyl-3- methylimidazolium hexafluorophosphate (BMIPF$_6$). Among the chemically modified graphene electrodes this value is quite high. Another significant of this electrode is that as the number of cycles increased capacitance increased continuously which is due to the oxygen functional groups residue of RGO.[32]

W.Y Tsai and coworkers in 2012 tested a supercapacitor using an electrode of KOH activated porous microwave exfoliated graphite oxide (a-MEGO) using a eutectic mixture of 1:1 ionic liquids i.e. N-methyl-N-propylpiperidinium bis(fluorosulfonyl)imide (PIP$_{13}$-FSI) and and N-butyl-N-methylpyrrolidinium bis(fluorosulfonyl)imide (PIP$_{14}$-FSI) as an electrolyte. After the optimization of carbon and electrolyte system a high capacitance of 180 F/g was achieved over a large potential window i.e. 3.5 V and over a unusual temperature window from -50 to 80° C. this was the first time that a carbon ionic liquid based supercapacitor exhibit the capacitance more than 100° C below room temperature. This shows that for the improvement of the capacitive energy storage one should optimize the carbon/electrolyte interface.[33]

In 2012 Y.J Kang and W Kim fabricate flexible solid-state supercapacitor by coating of CNT by using drip-dried method on office paper and ionic liquid gel electrolytes. Fumed silica Nano powder was mixed with 1-ethyl-3-methylimidazolium bis(trifluoro-methylsulfonyl)imide [EMIM-NTf$_2$] ionic liquid. This supercapacitor shows excellent cyclic stability up to 4000 charge/discharge cycle with less than 3% change in specific capacitance. Its specific capacitance was measured to be 135 F/g, energy density 41 Wh/kg and power density up to 164 kW/kg.[34]

M.F Al-Kady and R.B Kaner in 2012 fabricate graphene micro-supercapacitor using standard LightScribe DVD burner. Supercapacitors were fabricated over large area on graphite oxide

films by direct laser writing. An even sheet of polyethylene terephthalate (PET) was attached to the DVD disc surface, and a solution of GO is then drop cast on PET surface and dried within a night. For laser patterning the DVD disc is then inserted into the DVD optical drive using a computer software an integrated pattern was designed on GO film. Iongel was used as an electrolyte which was synthesized by mixing ionic liquid 1-butyl-3- methylimidazolium bis(trifluoromethylsulfonyl)imide [BMIM][NTf$_2$] and nan powder of fumed silica (FS) to form a clear viscous ion gel. Stacked micro supercapacitor with 16 integrated microelectrodes showed volumetric capacitance up to 2.35 F/cm^3 and the operating potential window also increased i.e. of 2.5 V and show increased cyclic stability i.e. capacitance remained unaltered even after 30,000 charge discharge cycles.[35]

Chapter: 3 Experimentation and Characterization Tools

In this research work Laser scribing technique is used to fabricate a low-cost supercapacitor. Commercial 200µm thick polyimide sheet is modified into porous graphene by using laser irradiations. The supercapacitor fabricated by this method is highly flexible, have high energy storage and fast charging and discharging cycle.

Apparatus Required for Electrolyte Preparation

Following apparatus is used to for the synthesis of ionic electrolyte i.e. 1-methyl-3-octylimidazolium bromide and 1-methyl-3-butylimidazolium bromide.

- Weight balance
- Hotplate
- Reflux
- Rotary evaporator
- Flask
- Beakers
- Glass rod stirrer
- Spactula

Materials Required

- 200 µm thick Polyimide sheet
- 1-methyl imidazolium
- Octyl bromide
- Acetonitrile
- Hexane
- Deionized water
- Ethanol

3.1. Fabrication of laser Scribed Supercapacitor

Polyimide is used a substrate material for the fabrication of flexible stacked supercapacitor. Polyimide is an insulating material which is reduced by laser irradiations and converted it into a conductive porous structure. For stack type supercapacitor Polyimide sheet is cut into 2x3 cm rectangles and then washed with deionized water.

Laser engraver of 450nm wavelength (maximum power 500mW) is switched on and connected to the computer. Computer has a software installed to control the distinctive features of laser engraver e.g. moving the stepper motor in XY direction to adjust the laser source, import images for writing, rotate or reverse the image, laser power and carving time. Laser engraver is first optimized to get the required result i.e. to get the carbonized structure with high conductivity, continuous and fine structure. For stacked capacitor a square box of 1x1 cm dimension was drawn by MS paint and then the image was imported into the laser software. Two electrodes are needed for making a single supercapacitor device. Polyimide sheet is then placed on the stage under the laser source and image is then scribed on the polyimide sheet to obtain the carbonized structure which is called laser induced graphene (LIG). To connect these electrodes with external measuring instruments connecting electrodes are needed so an additional area of 0.2x1 cm was reduced with laser which is connected to the 1x1cm square box.
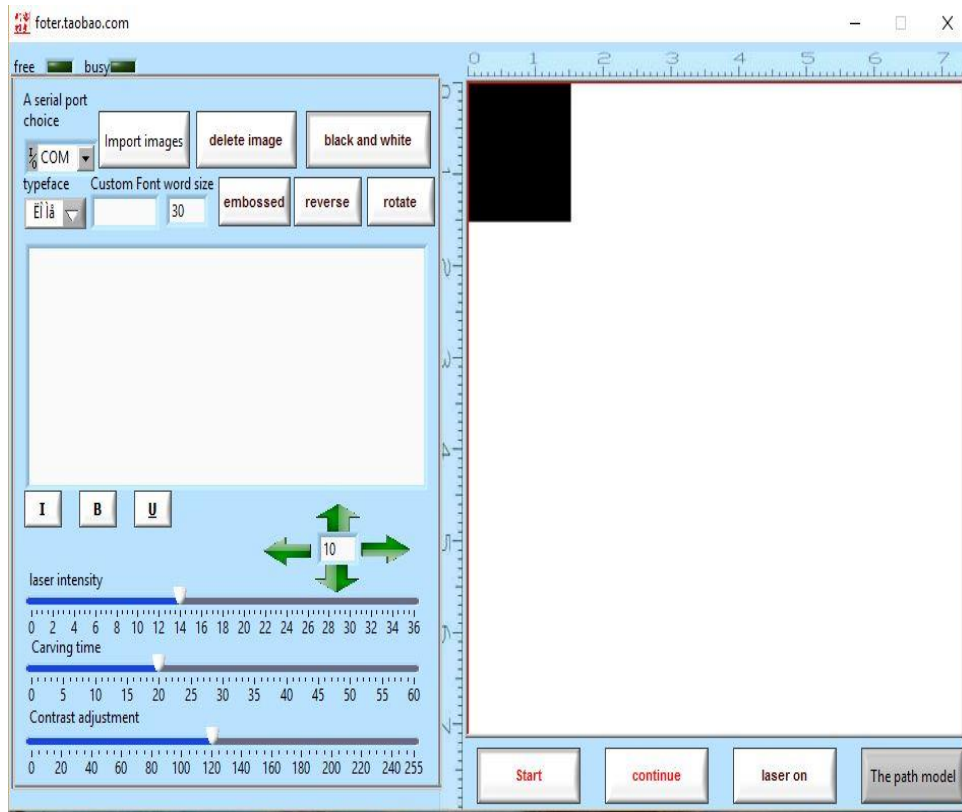
Figure 6(a) Laser software on computer with electrode drawn on it (b) Laser scribed PI sheet with 1x1cm electrode's dimension and connecting electrodes
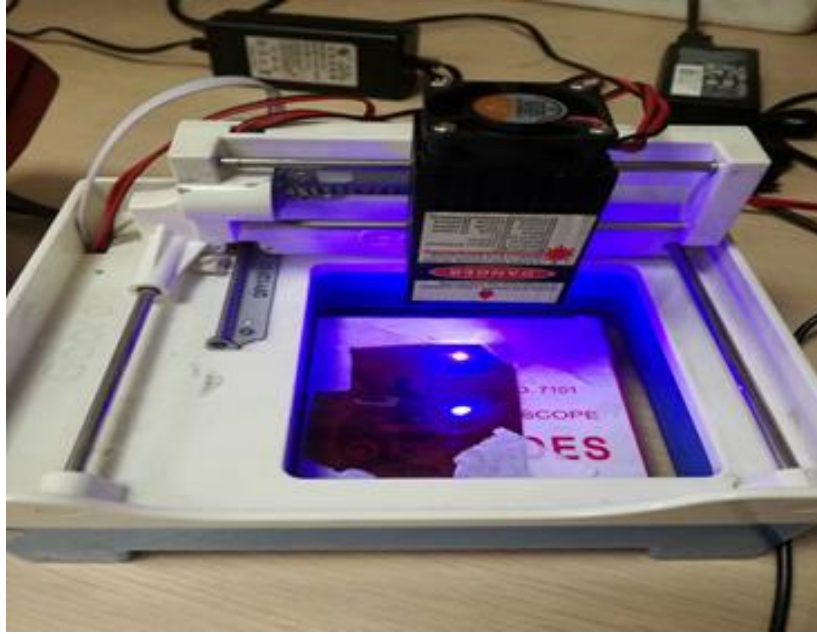
Figure 7 Laser machine during electrode formation of electrode

3.2. Electrolyte Preparation

Electrolytes have been an important key component in the performance of supercapacitors. The ideal electrolytes we are looking for must have a wider potential window, high ionic conductivity, high chemical and thermal stability, cost effective and environment friendly. Electrolytes cannot meet all these requirements so we must choose an electrolyte which have less shortcomings and gives us high performance supercapacitors. There are several types electrolytes, they are divided into three main categories and then further divided into sub categories as shown in figure 3.6
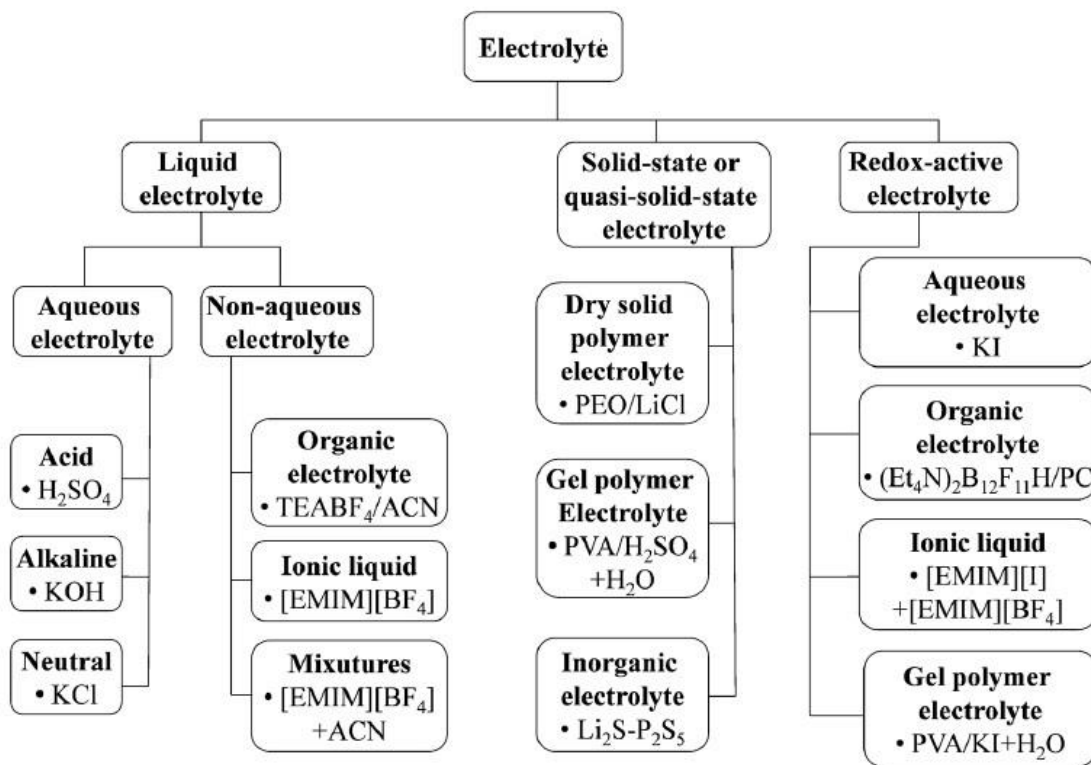
Fig 3.1 Classification of electrolytes for supercapacitors.

Capacitance, energy and power density as well as the charge discharge cycles of a supercapacitor depends upon the nature of an electrolyte which include following factors.

- Nature and size of ion
- Ion and solvent concentration
- Ion solvent interaction
- Electrolyte and electrode material interaction
- Electrolyte potential window

Here in this research we use ionic electrolyte to check our device performance as ionic liquid electrolytes provides high voltage window which helps to enhance the energy and power density of a supercapacitor.[36]

3.2.1. Ionic Liquid (IL) Electrolytes

Ionic liquids (ILs) are molten salts at room temperature, these salts are only composed of ions and have low melting point i.e. 100° C. Typically ILs comprise of a large symmetric organic cation and a weakly arrange organic or inorganic anion. Ionic liquids drawn so much attention

due to their unique structure and properties. ILs have high thermal and chemical stability, low vapor pressure and are generally noninflammable. ILs have highly tunable physical and chemical properties. Recent studies show that supercapacitors having ILs electrolytes have significantly high operative voltage i.e. higher than 3V. ILs are also termed as solvent free electrolytes because they only consist of salts and don't contain volatile organic compounds.

Generally, there are two mostly used and potential families of aprotic ionic liquids which have been considered most promising for supercapacitors. These families commonly based on pyrrolidinium and imidazolium cations. Commonly pyrrolidinium cations based ILs possess high electrochemical stability which means they have high operating voltage, while ILs based on imidazolium cation have higher conductivity and low viscosity than the former. These properties enable imidazolium based ILs to have fast charge discharge conditions.[36, 37]

Here we synthesize imidazolium based ionic liquid electrolyte, the synthesis procedure is given as follows.

Preparation of 1-Methyl-3-Octylimidazolium Bromide

1-methyl 3-octylimidazolium is obtained by making a solution of 1-methyl Imidazolium 5g (60 mmol) and octyl bromide 12.19g (60 mmol). This solution was then refluxed in 30ml of acetonitrile for 48 hours at 90°C. 1-methyl-3-octylimidazolium bromide was decanted from the hot solution into a flask. The solution is then washed using hexane. The residue is then dried in a rotary evaporator at 45°C under reduced pressure to obtain methyl-3-octylimidazolium bromide (90%). The formed product was characterized by FTIR and NMR and was found pure.

Preparation of 1-Methyl-3-Butylimidazolium Bromide

1-methyl 3-butyl imidazolium is obtained by making a solution of 1-methyl Imidazolium 5g (60 mmol) and butyl bromide 8.214g (60 mmol). This solution was then refluxed in 30ml of acetonitrile for 48 hours at 90°C. 1-methyl-3-octylimidazolium bromide was decanted from the hot solution into a flask. The solution is then washed using hexane. The residue is then dried in a rotary evaporator at 45°C under reduced pressure to obtain methyl-3-butylimidazolium bromide (90%). The formed product was characterized by FTIR and NMR and was found pure.

3.3. Assembly of Stacked Supercapacitor

Taking the laser reduced electrodes and ionic electrolytes a supercapacitor was assembled very carefully. The basic structure of the device is that we sandwiched the electrolyte and a separator between the laser scribed electrodes i.e. it is a rPI/ionic electrolyte/rPI structure. A uniform layer of 1-methyl 3-octyl imidazolium bromide ($[C_8mim]$ Br) is pasted on both electrodes with a spactula and then a filter paper with pore size 0.6µm and dimensions of 1x1cm is placed between the both electrode and these electrode is then stacked together using a paper clip so that there will be no airgap between them and connecting electrodes are exposed to connect it with different measuring instruments. Using the same procedure another supercapacitor is made but using 1-methyl 3-butyl imidazolium bromide ($[C_4mim]$ Br) as an electrolyte we then compare the capacitance values of both electrolytes.
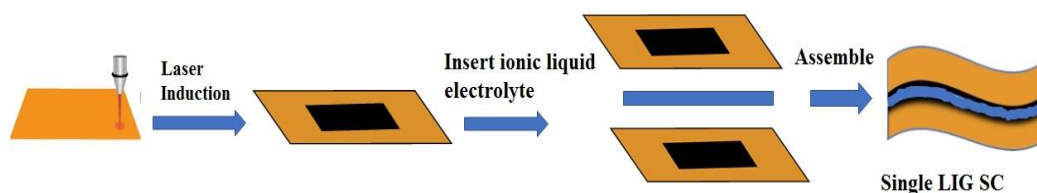

Figure 3. Schematic illustration of the fabrication and assembling process of single LIG-SC

3.4. Characterization Technique

3.4.1. Fourier Transform Infrared Spectroscopy (FTIR)

Infrared spectroscopy is used to identify certain functional groups present in a molecule. It is also called functional group spectroscopy. We can do a functional group analysis of any chemical compound. Chemical nature of a given compound can be identified from the mode or transition and absorption. We can also detect impurities or purity of a compound from unique set of absorption bands. Working principle of infrared spectroscopy is rely on the fact that the internal vibration's frequencies of a certain molecule is unique, but only those frequencies are observed

in FTIR which occur in the infrared region of electromagnetic spectrum i.e. ~ 4000 cm^{-1} to ~ 200 cm^{-1}.

In FTIR when the low energy infrared radiations interact with the matter. The sample will only absorb the radiation frequency that corresponds to its vibrational and rotational frequencies while all the other frequencies will be transmitted. The absorbed frequencies of infrared radiations are then measured by an infrared spectrometer and a graph of absorbed energy vs frequency is plotted and infrared spectrum of a material is obtained. We can identify a material from its infrared spectrum because every material has a distinct infrared spectrum. We can also determine the presence of certain chemical groups in a chemical structure from the absorbed frequencies. Concentration of a specie can be calculated using FTIR from the magnitude of radiations absorption of that specific specie.

The infrared spectrum is obtained by passing infrared light through the sample. The IR radiations from the source pass through an interferometer that regulates the radiations. It performs an optical inverse Fourier transforms on the entering radiations. The different wavelength of regulated infrared beam is then absorbed by the various molecules present in the sample. The molecules of the sample will show vibrational and rotational motion of the frequency of the incident radiations matches with frequency of the chemical bond exist in the sample. The absorbed intensity of the IR beam is detected by the detector. Detector measures the change in energy of the absorbed radiations by the sample. The signal from the detector is then processed by the computer and we get the IR spectrum of the given sample.[38, 39]

The basic components of infrared spectrophotometry are

   i.   Source of infrared light
  ii.   Interferometer
 iii.   Sample
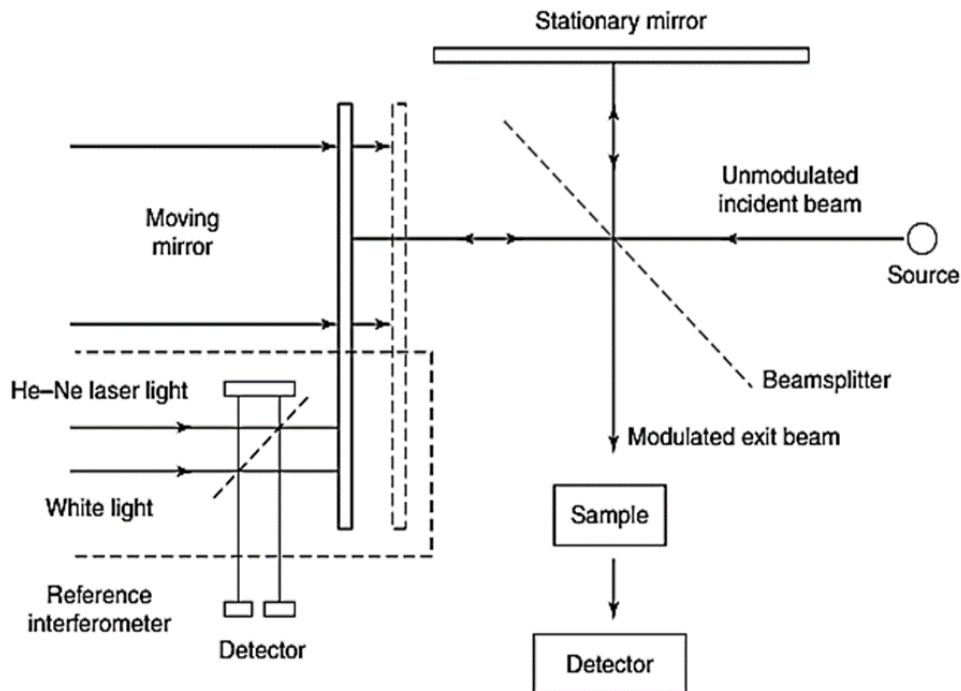 iv.   Detector
   v.   Computer

Fig. 3. Schematic diagram of working of FTIR spectrophotometer [40]

3.4.2. X-Ray Diffraction (XRD)

X-ray diffraction (XRD) is an analytical technique which is non-destructive which utilizes the wave particle nature of X-ray to determine crystallinity, composition and the lattice constants of any substance. Diffraction pattern is used to characterize a compound.

XRD works on the principle of Bragg's Law. The monochromatic radiations when interact with the material they produce constructive interference and satisfying Bragg's condition i.e.
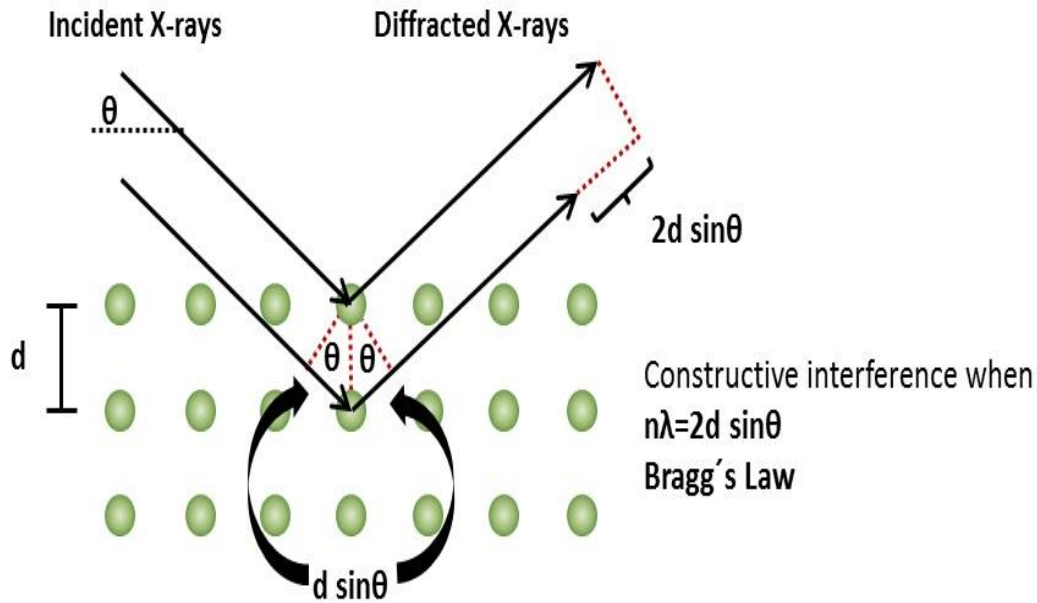
$$n\lambda = 2dsin\theta$$

Figure.4. X-ray diffraction by planes of crystal.

X−ray diffractometers comprised of three basic components. X-ray tube, sample holder and X-ray detector. A cathode ray tube which generates the X-rays by heating the filament which caused electrons to accelerate. These electrons having sufficient energy displace the inner shell electrons of the target material we get a characteristic X-ray spectrum. When a beam of monochromatic X-rays falls on the target material we get an interference pattern from that material. Cathode ray tube generates the X-rays and these radiations are modified and directed on the sample. We get the interference pattern as soon as the X-rays interact with the sample. The diffraction pattern is then processed. The sample is scanned over a range of 2θ angles. Every material has a unique size and shape of a unit cell so the direction of the possible diffraction will be different for every material. The diffraction pattern tells us about the crystallinity, phase and purity of a sample. Using XRD we can also determine unit cell dimensions, dislocations and lattice mismatch.[41]
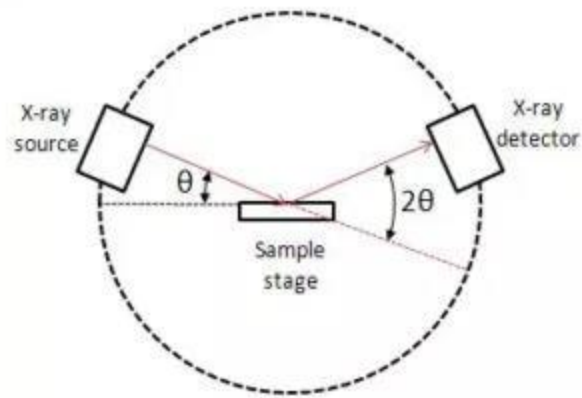
Figure.5. Schematic diagram of XRD.

3.4.3. Scanning electron microscope (SEM)

Scanning electron microscope (SEM) is characterization technique which is utilized to investigate the composition and surface morphology of the sample. A focused beam of high energy electrons falls upon the surface of the specimen and variety of signals are generated. These signals are then collected by the detectors to form images on computer. These images then give us information about the crystal structure, morphology and chemical composition of the material. Maximum SEM resolution is 1-20nm.

SEM Components

SEM consists of following components

- ➢ Electron Gun
- ➢ Electromagnetic lenses
- ➢ Magnetic Scanning coils
- ➢ Sample holder
- ➢ Detectors
- ➢ Computer

SEM Working

When a focused electron beam falls on the surface of a specimen. The electron beam inspects the surface of the specimen, after the interaction of electrons with the sample releases the secondary electrons, backscattered electrons and characteristic X-ray are produced. All these signals are then focused on the detector to form images on the computer screen. The accelerating voltage of

Figure 8 (a) Schematic diagram of interaction of electron beam (b) SEM construction.
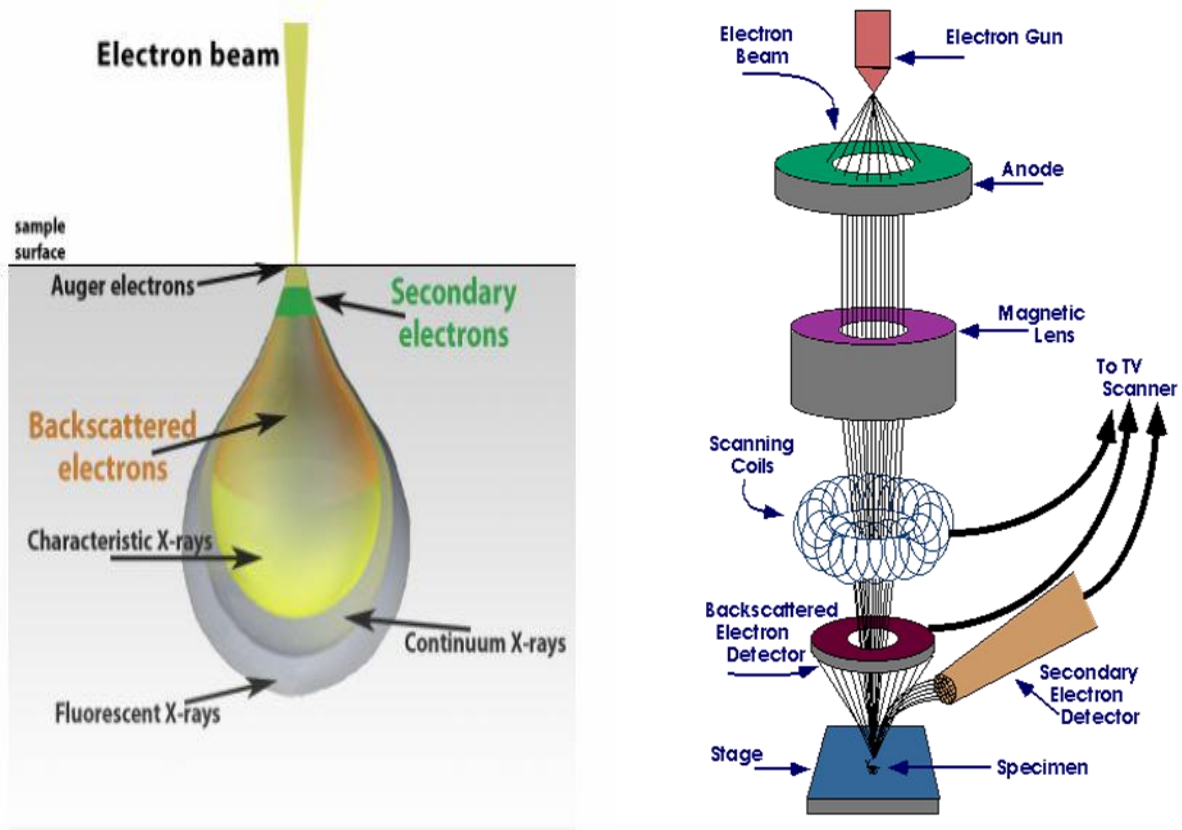
electrons and density of the sample will decide how deep the electrons will penetrate the sample mostly it is up to few microns.

Secondary electrons are the common mode of detection in SEM. A clear image of the sample can be obtained from the electrons which are emitted near the surface of the specimen. Elastic and back scattering of the electrons also produced they immerge when they interact with the deeper location and that is why their resolution is low as compared to secondary electrons. When the inner electrons knocked out from the shell characteristic X-rays produced. All these signals are detected by detectors and images then formed on the computer screen with the help of which we can investigate the morphology, crystallography and planes orientations.[42]

3.4.4. Electrochemical Workstation

Electrochemical testing for supercapacitor devices can be done by using an electrochemical workstation. EC-lab software and ECI workstation has been used for measuring electrochemical properties of our device. It provides several techniques like cyclic voltammetry (CV), linear sweep, differential pulse and square wave voltammetry, impedance spectroscopy and chronoamperometry can also be perform using EC-lab software. It is a window based software having tools like integrated digital CV simulator, impedance simulation and fitting program and all these tools are of key importance to understand kinetics reaction, trace level analysis, corrosion, energy storage and energy conversion mechanisms. Cyclic voltammetry technique gives information about the electrode and electrolyte interface. This software is designed for the testing of SC and Lithium ion batteries.

Cyclic Voltammetry (CV) is a technique which is widely used to analyze quantitative information regarding electrochemical reactions. CV gives information on adsorption processes, mixed electron transfer reactions and redox reactions. It shows abrupt locations of redox potentials of the electroactive species. The CV technique study the potential of a working electrode by applying triangular potential waveform. During the process of changing potential, electrochemical reactions producing current which occurred between the electrode and electrolyte interface is measured by the potentiostat and successive the applied potential. The cyclic voltammogram plots the reaction of the material's or device current as a function of the applied potential. Traditionally, this approach is used performing an analog ramp. Due to the digital nature of the potentiostat, the actual applied ramp consists in a series of small potential steps that approximate the targeted linear ramp. This technique corresponds to normal cyclic voltammetry, using a digital potential step i.e. it runs clearly defined potential increments at regular intervals of time. The software adjusts the potential steps (composing the increment) to be as small as possible.

This technique consists of following steps

- ➢ a starting potential setting block,

- ➢ a 1st potential sweep with a final limit E1,

- ➢ a 2nd potential sweep in the opposite direction with a final limit E2,

- ➤ the possibility to repeat n_c times, the 1st and the 2nd potential sweeps,

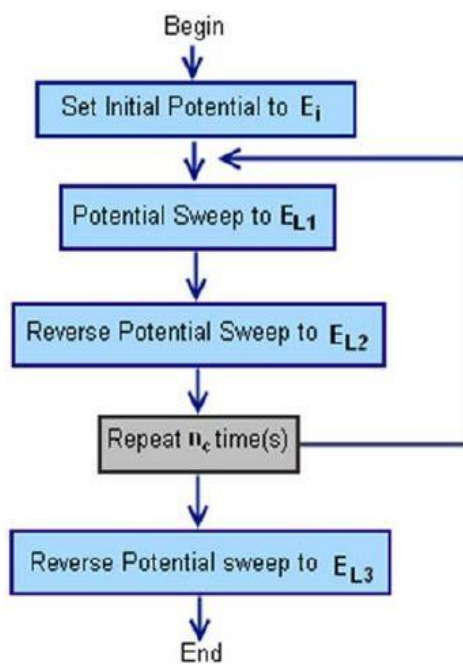- ➤ a final conditional scan reverse to the previous one, with its own limit EF

Figure 9 General diagram of cyclic voltammetry.

Figure 10 Detailed column diagram of cyclic voltammetry.

Figure 11 EC workstation in surface lab of SCME (NUST) Islamabad, which is used for measuring CV for our IL based SC.

EC-lab software controls all the instruments including standard electrochemical techniques i.e. CV, potentiometry, amperometry, pulsed technique and electrolysis etc. along with monitoring also analyze with the help of tools such as Z Fit (EIS data modeling), CV Fit (voltammetry fitting).

Chapter 5: Results and Discussion
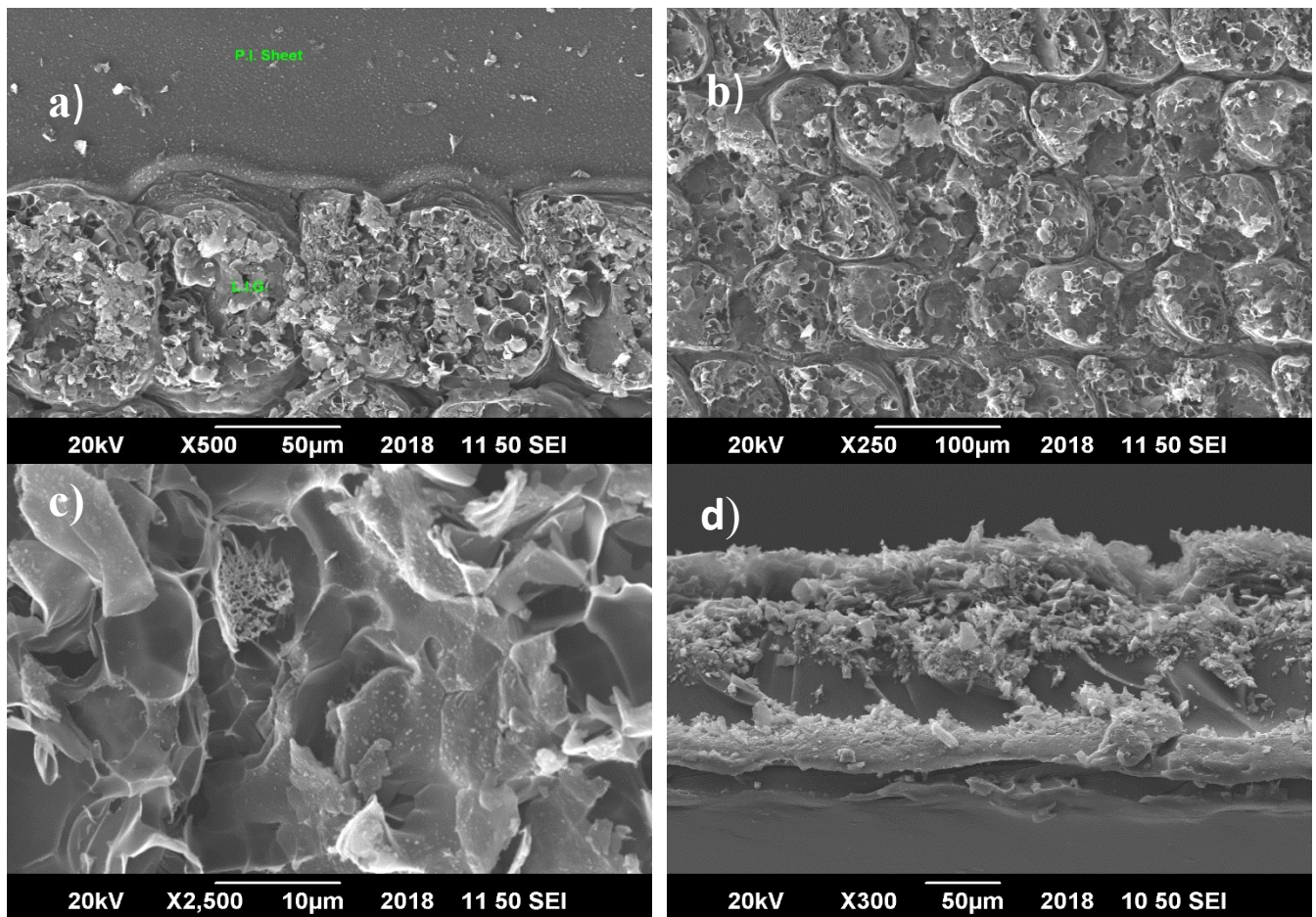
5.1. Scanning Electron Microscope

Figure 12 SEM images of LIG. Top view SEM images a, b and c (d) is cross sectional SEM image All images are taken from samples at laser power 138mW

The various SEM images of LIG are shown in figure 5.1. In figure 5.1 b and c we can clearly see the change in morphology of PI sheet. PI sheet after laser scanning converted into the carbonized structure in figure 5.1a we can clearly see the morphological change between PI sheet and PI sheet after laser irradiation i.e. LIG. Figure 5.1b shows the ordered porous structure which shows the uniform and constant laser exposure it and this porous morphology formed due to the release of some gaseous products. This interconnected porous structure is a evidence of the good conductance of the electrode as charge flow become uninterrupted because of such structure.

Figure 5.1c shows that inside the carbonized structure development of micro-scale pores and it also suggest the formation of nanoscale carbon sheets. Figure 5.1d is the cross-sectional view of SEM image of porous morphology of LIG, after laser exposure formation of ordered porous structure increases the accessible surface area which in return enhance the penetration of electrolyte on the electrode material.[43-45]

5.2. X-Ray Diffraction (XRD)

Figure 13 XRD of PI (Top) and LIG (Bottom)
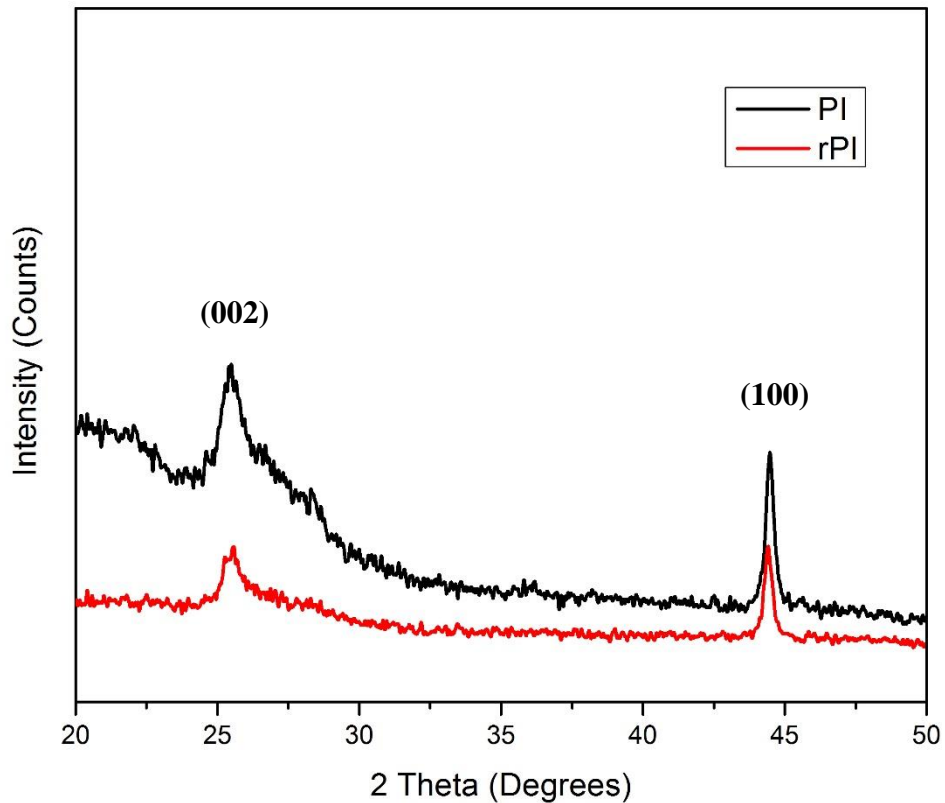
Figure.2 shows the XRD results of Polyimide sheet (PI) and polyimide sheet after laser reduction i.e. LIG. The XRD peak of PI and LIG was observed at angle 25.5^o but for LIG the XRD peak reduced which confirms the carbonaceous structure and high degree of graphitization. These results showed that in the conducting layer there are short range order carbon rich clusters which

makes our device suitable for energy storage. The reduction in the XRD peak of rPI indicates the distortion in crystallinity. XRD peak at plane (002) confirms the high degree of graphatization [45, 46]

5.3. Fourier Transform Infrared Spectroscopy
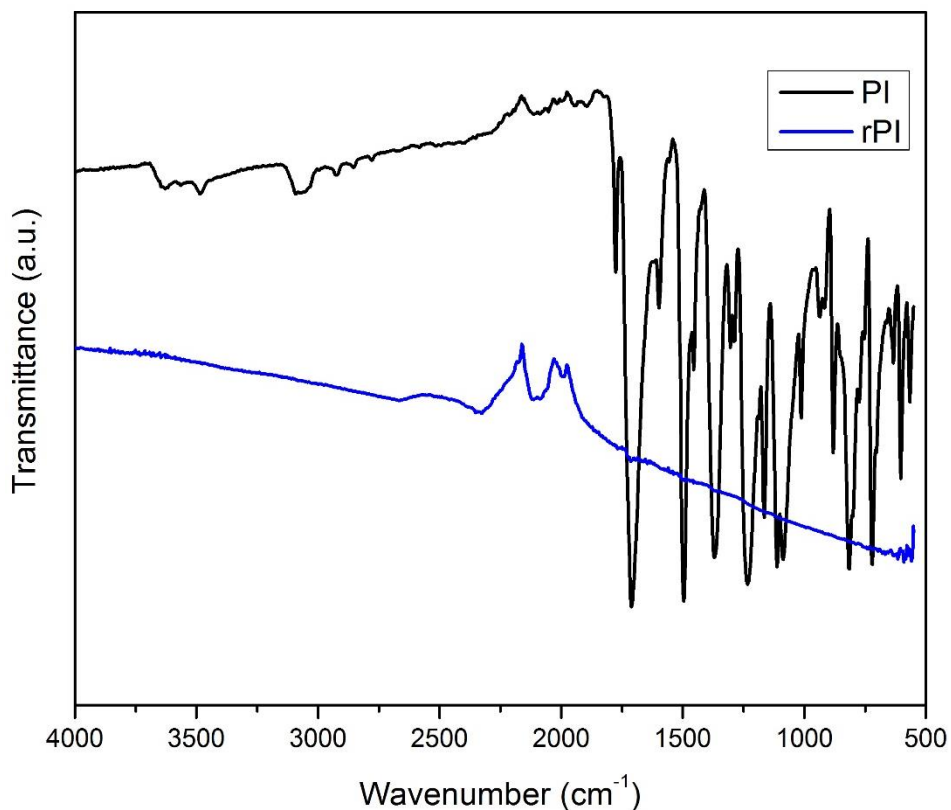
Figure 14 FTIR spectra of PI sheet and LIG

Figure.3 shows the FTIR spectra of PI sheet and LIG. Distinct peaks 723 -1776 cm^{-1} are observed which are the perfect match with the FTIR results of commercial PI. In the FTIR spectra for PI sheet we observed the peaks at 1776 cm^{-1} which shows the asymmetric stretching vibrations of the C=O and at 1710 cm^{-1} which shows the C=O symmetric stretching vibrations of imide adsorption band. The peak at 1370 cm^{-1} is because of the C—N stretching mode and peak at 723 cm^{-1} indicate bending modes of C=O of imide group. The FTIR spectra of LIG showed a broad absorption of peaks from 720-800 cm^{-1} which indicated variation of chemical

structure. This indicates that after laser treatment the chemical bonds are broken in PI as the gaseous products are released after laser irradiations converting the surface of PI film into conducting carbon rich clusters.[45-47]
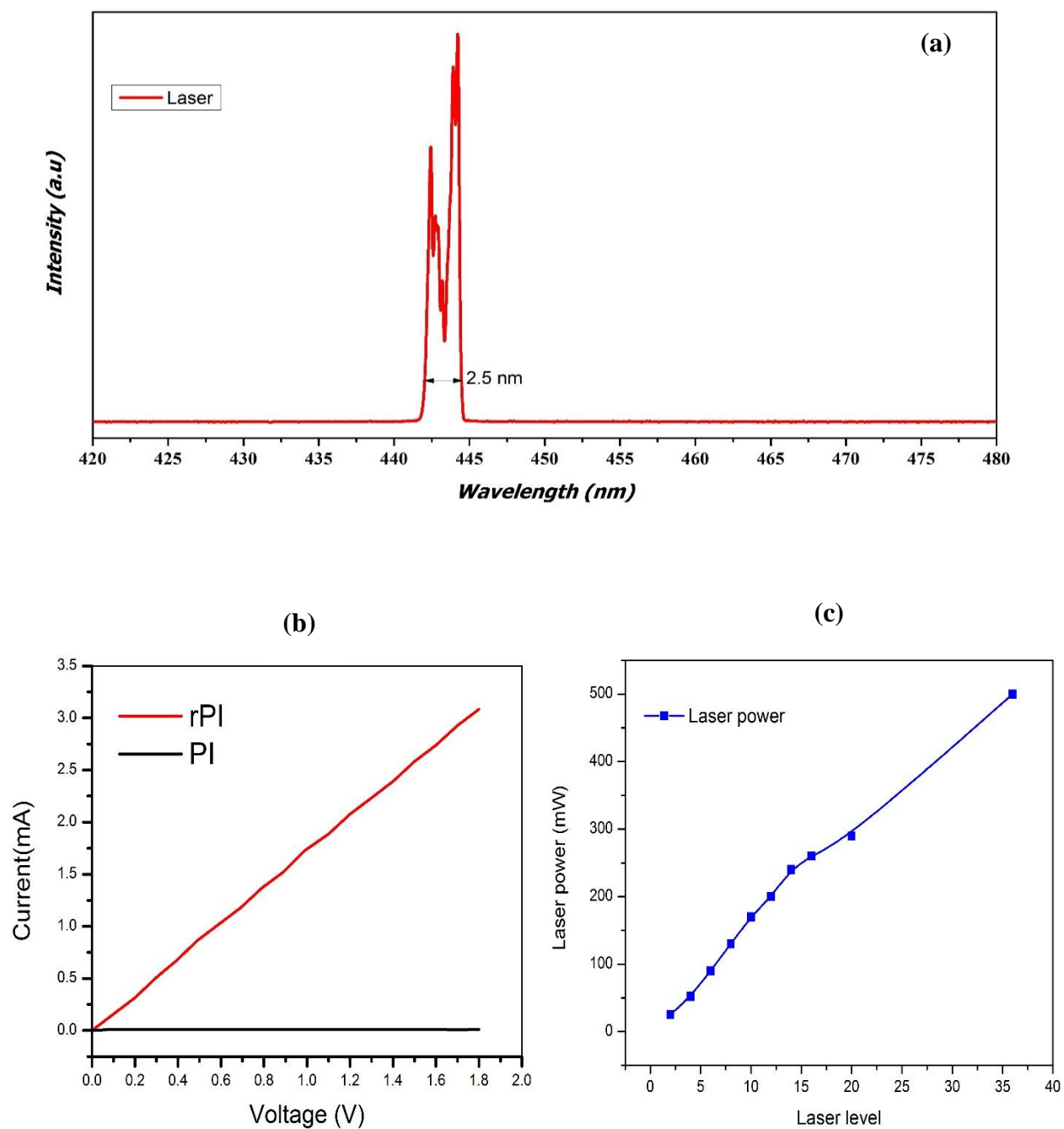
5.4 Laser Characterization

Figure.4a shows the laser wavelength graph. The laser wavelength was determined at National Center for Physics Islamabad, In Laser Plasma Physics Lab. The wavelength of the laser we used in experiments was measured to be 440-44nm which shows that it is solid state laser with blue light which lies in UV region of electromagnetic spectrum.[48] Figure. 4b is the conductivity graph of PI and rPI it shows that rPI shows good conductive behavior i.e. a linear graph giving a maximum current output 3.2 mA when a voltage sweep of 0-2V is applied, which confirms the transformation of PI insulator into rPI conductor after laser treatment. Figure. 4c shows the laser power graph vs laser intensity levels available in laser software where changing these levels we can change the laser power. The maximum power of the laser was measured to be 500mW.

Figure 15 (a) Laser wavelength graph, (b) PI and rPI conductivity graph (c) Laser power vs Intensity graph

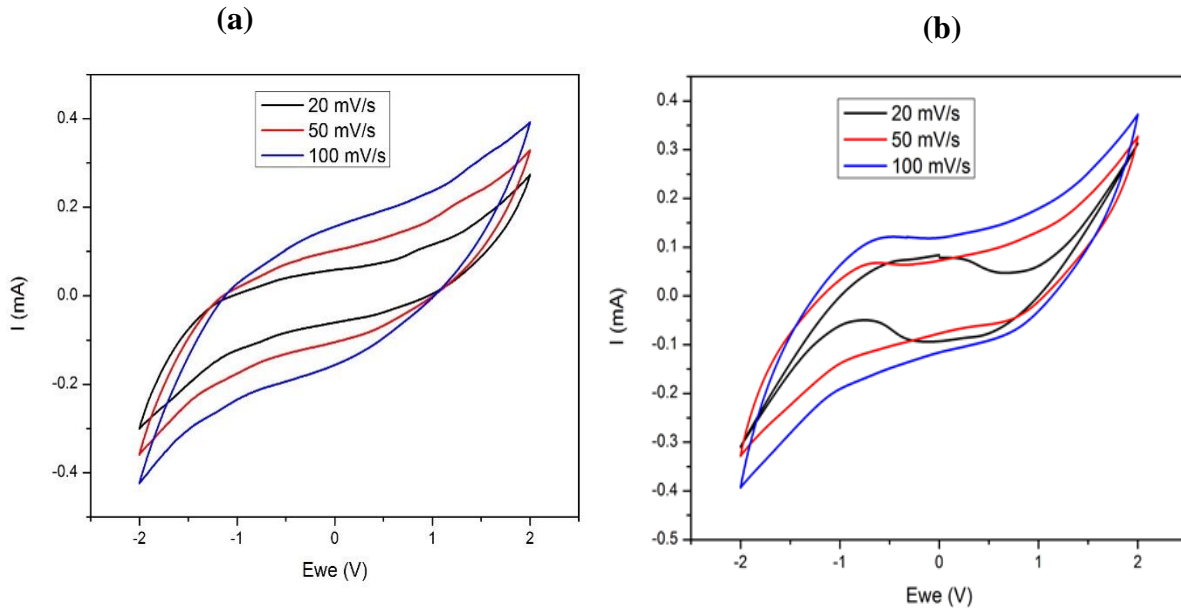## 5.4. Cyclic Voltammetry (CV) and Galvanostatic Charge Discharge (CC)

Figure 16 CV curve of LIG-SC with IL (a) ([C4mim] Br) and (b) ([C8mim] Br) at various scan rates

Electrochemical testing results testing results of laser scribed SC devices at different scan rates is shown in Figure.4. The value of specific capacitance (C_A) is calculated by using different electrolytes using the LIG as an electrode for all those electrolytes. The value of (C_A) for IL ([C_4mim] Br) is calculated to be 313 µF/ cm^2, 24 µF/ cm^2 and 1.65 µF/ cm^2 at scan rate of 20, 50 and 100 mV/s respectively while the C_A for IL ([C_8mim] Br) is calculated to be 3.8 mF/ cm^2, 1.76 mF/ cm^2 and 1 mF/ cm^2 at the scan rate of 20, 50 and 100 mV/s. The CV curve of these ILs is quasi-rectangular which shows good EDLC behavior of our capacitor. This CV curve also shows that there is no redox reaction occur as there are no anodic and cathodic peaks representing ideal EDLC behavior.[45]

It is observed here that by increasing the scan rate the value of specific capacitance decreases. It is because at lower scan rate the electrolyte has greater contact with the surface of electrode material and it also allow the complete peforation of the electrolyte into the e pores of electrodes resulting in the greater charge storage on electrode surface.[49]
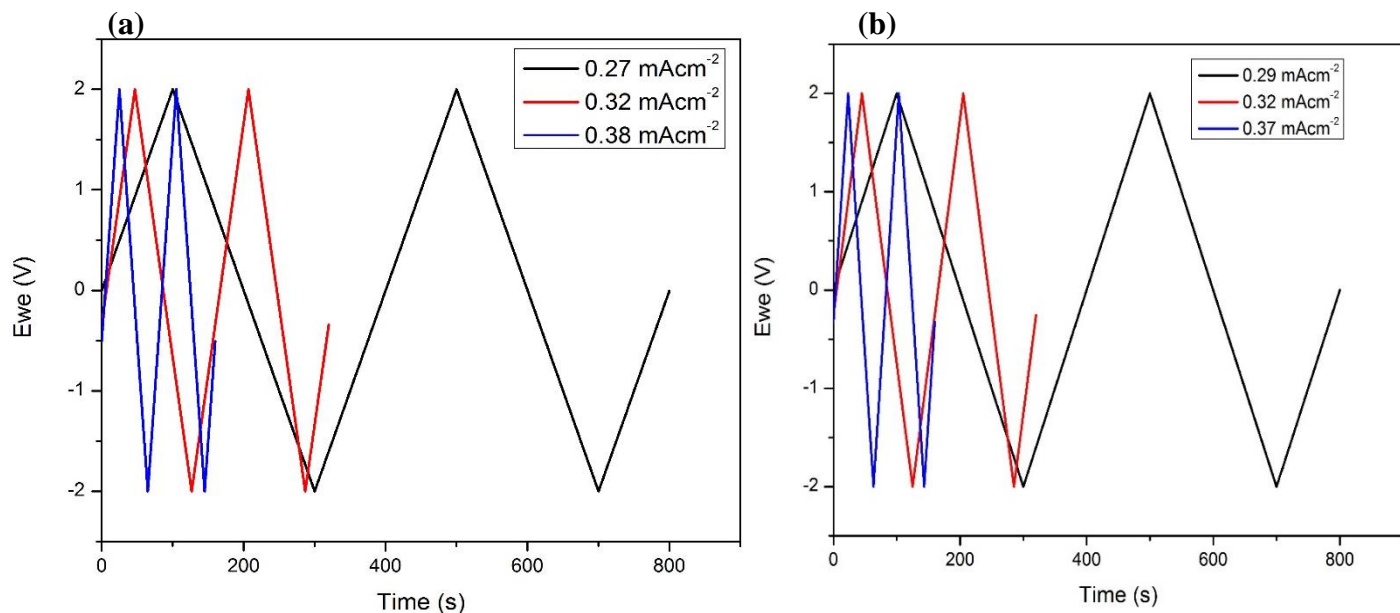
Figure 17 galvanotactic charge discharge CC curves for (a) ([C4mim] Br) and (b) ([C8mim] Br) ionic liquid

The galvanotatic charge discharge curve (CC) of ionic liquid ([C_4mim] Br) and ([C_8mim] Br) demonstrated in Figure.5 (a) and (b) respectively. The CC curve in Fig. 5a shows that when different current densities i.e. 0.27 and 0.32 and 0.38 mA/cm^2 were applied this CC curve shows good capacitive behavior because this curve is a perfect rectangle. Similarly, for ionic liquid ([C_8mim] Br) the CC curve is also almost triangular showing good capacitive behavior by applying different current densities e.g. 0.29, 0.32 and 0.37 mA/cm^2 to the device. It is also noted in this CC graph that for low current densities the charge discharge time increases and for high current densities it decreases this may be the result of fast variation in potential which cause less penetration of electrolytic ions into the electrode's pores.[50, 51]
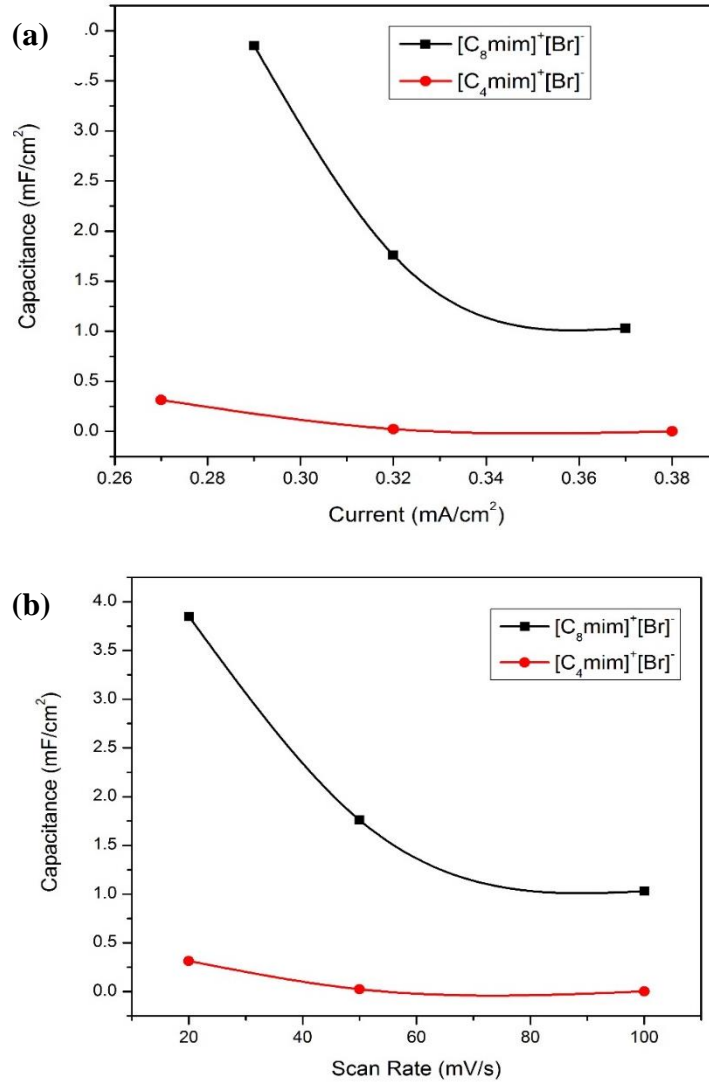
Figure 18 Graph for (a) Capacitance vs current density and (b) Capacitance vs scan rate for IL ([C4mim] Br) and ([C8mim] Br)

Figure. 6a shows the specific capacitance C_A and current density graph for ([C$_4$mim] Br) and ([C$_8$mim] Br) ILs. For ([C$_8$mim] Br) the graph shows the abrupt decrease in the capacitance as current density increases but for ([C$_4$mim] Br) it shows a very small decrease in C_A as current density increases. Drop in the C_A with increasing current density is because of the increase in the potential drop which is caused by the material's resistance. The surface area of electrode's structure is more approachable to the ions of electrolytes when the current density value is low resulting in higher value of C_A.[52] In Figure. 6b there is graph of C_A vs scan rate. It is observed that increasing scan rate cause the C_A to decrease. The value of (C_A) for IL ([C$_4$mim] Br) at scan rate 20 mV/s is calculated to be 313 µF/ cm^2, at scan rate of 50 mV/s it is 24 µF/ cm^2 and at 100 mV/s it is 1.65 µF/ cm^2 while for the IL ([C$_8$mim] Br) is C_A at 20 mV/s is 3.8 mF/ cm^2, at 50

mV/s it is 1.76 mF/ cm^2 and at 100 mV/s it is calculated to be 1 mF/ cm. The reason we find this trend is because electrolyte can penetrate more into the pores by with low scan rate and it also allows the electrolyte ion to diffuse more onto the electrode internal structure so the more charge can be stored on the electrode's surface resulting higher value of C_A. as for high scan rate the contact between the electrolyte ions and electrode is for a very small amount of time the electrolyte ions diffusion onto the electrode surface become difficult resulting in the less charge storage on the surface of electrode that is why low C_A is observed.[49]

Calculations

The formulas that has been used for the calculations of the capacitance of the supercapacitors are listed below,

$$C_{device} = \frac{I}{\frac{dV}{dt}} \qquad (1)$$

$$C_{area} = \frac{C_{device}}{A} \qquad (2)$$

OR

$$C_A = \frac{1}{2 \times S \times (v_f - v_i) \times \frac{dV}{dt}} \int_{v_i}^{v_f} I(V) dV \qquad (3)$$

These three equations are used to calculate and confirm the capacitance value of the device.

Here, the average current density id represented by I which is in mA, and $\frac{dV}{dt}$ is scan rate measured in mV/s, and A and S in equation. 2 and 3 respectively, represents the area of device in cm^2 and $(V_f - V_i)$ are the voltage limits applied to the device.[44, 45]

Conclusion

Supercapacitors were fabricated using laser scribing technique, an optimum laser power 138mW was used to reduce the polyimide (PI) sheet converting it to reduced polyimide (rPI) a conducting electrode material which is perfect for supercapacitor (SC) applications. Laser irradiations convert the non-conductive PI sheet into a conducting carbonaceous and porous structures these pores are interconnected which is a result of continuous laser exposure and significant for charge flow. In this work 1-methyl 3-octyl imidazolium bromide ([C$_8$mim] Br) and 1-methyl 3-butyl imidazolium bromide ([C$_4$mim] Br) ionic liquids (ILs) electrolytes were sandwiched between rPI electrode. The maximum areal capacitance was up to 3.8mF/cm^2 for ([C$_8$mim] Br) and 313µF/cm^2 for ([C$_4$mim] Br) IL electrolyte. These electrolytes showed good capacitance stability over time as the galvanostactic charge discharge curve (CC) was triangular which makes them potential candidate for energy storage application. An easy and inexpensive fabrication technique and a commercially easily available substrate was used in this work for the fabrication of ILs based SC which give us good capacitance value. Capacitance value can be improved by further optimization of laser power and some other ionic liquids can also be tested with greater chain length and high conductivities. Controlling laser power stacked series and parallel SC can also be fabricated with different electrolytes and can be further tested to check their performance.

References

[1]   M. A. Monne, X. Lan, and M. Y. Chen, "Material Selection and Fabrication Processes for Flexible Conformal Antennas," *International Journal of Antennas and Propagation,* vol. 2018, 2018.

[2]   T.-H. Han, H. Kim, S.-J. Kwon, and T.-W. Lee, "Graphene-based flexible electronic devices," *Materials Science and Engineering: R: Reports,* vol. 118, pp. 1-43, 2017/08/01/ 2017.

[3]   T. Russell, B. Baron, D. Brestovansky, P. Lutz, and R. Rocheleau, "Properties of continuously-deposited photovoltaic-grade CdS," in *Conf. Rec. IEEE Photovoltaic Spec. Conf.;(United States)*, 1982.

[4]   W. S. Wong and A. Salleo, *Flexible Electronics: Materials and Applications*: Springer US, 2009.

[5]   D. B. Mitzi, L. L. Kosbar, C. E. Murray, M. Copel, and A. Afzali, "High-mobility ultrathin semiconducting films prepared by spin coating," *Nature,* vol. 428, p. 299, 2004.

[6]   P. T. Kazlas and M. D. McCreary, "Paperlike microencapsulated electrophoretic materials and displays," *MRS bulletin,* vol. 27, pp. 894-897, 2002.

[7]   M. Yan, T. W. Kim, A. G. Erlat, M. Pellow, D. F. Foust, J. Liu*, et al.*, "A transparent, high barrier, and high heat substrate for organic electronics," *Proceedings of the IEEE,* vol. 93, pp. 1468-1477, 2005.

[8]   N. G. McCrum, C. Buckley, C. B. Bucknall, and C. Bucknall, *Principles of polymer engineering*: Oxford University Press, USA, 1997.

[9]   E. Jamieson and A. Windle, "Structure and oxygen-barrier properties of metallized polymer film," *Journal of Materials Science,* vol. 18, pp. 64-80, 1983.

[10]   K. Long, A. Kattamis, I.-C. Cheng, H. Gleskova, S. Wagner, and J. Sturm, "Stability of amorphous-silicon TFTs deposited on clear plastic substrates at 250/spl deg/C to 280/spl deg/C," *IEEE Electron Device Letters,* vol. 27, pp. 111-113, 2006.

[11]   H. Chatham, "Oxygen diffusion barrier properties of transparent oxide coatings on polymeric substrates," *Surface and Coatings Technology,* vol. 78, pp. 1-9, 1996.

[12]   W. Liu, D. Lin, A. Pei, and Y. Cui, "Stabilizing lithium metal anodes by uniform Li-ion flux distribution in nanochannel confinement," *Journal of the American Chemical Society,* vol. 138, pp. 15443-15450, 2016.

[13]   C. E. Sroog, "Polyimides," *Journal of Polymer Science: Macromolecular Reviews,* vol. 11, pp. 161-208, 1976.

[14]   K. Subramani and W. Ahmed, "Fabrication of PEG Hydrogel Micropatterns by Soft-Photolithography and PEG Hydrogel as Guided Bone Regeneration Membrane in Dental Implantology," in *Emerging Nanotechnologies in Dentistry*, ed: Elsevier, 2012, pp. 171-187.

[15]   K. Chen, Q. Wang, Z. Niu, and J. Chen, "Graphene-based materials for flexible energy storage devices," *Journal of Energy Chemistry,* 2017.

[16]   Y. Wang, Z. Shi, Y. Huang, Y. Ma, C. Wang, M. Chen*, et al.*, "Supercapacitor Devices Based on Graphene Materials," *The Journal of Physical Chemistry C,* vol. 113, pp. 13103-13107, 2009/07/30 2009.

[17]   J. Zhu, D. Yang, Z. Yin, Q. Yan, and H. Zhang, "Graphene and graphene-based materials for energy storage applications," *Small,* vol. 10, pp. 3480-3498, 2014.

[18]   L. Jiao and R. Gorby, "Laser scribed graphene for energy storage application," in *Opto-Electronics and Communications Conference (OECC), 2015*, 2015, pp. 1-3.

[19]   M. Vangari, T. Pryor, and L. Jiang, "Supercapacitors: review of materials and fabrication methods," *Journal of Energy Engineering,* vol. 139, pp. 72-79, 2012.

[20] J. Libich, J. Máca, J. Vondrák, O. Čech, and M. Sedlaříková, "Supercapacitors: Properties and applications," *Journal of Energy Storage,* vol. 17, pp. 224-227, 2018.

[21] Z. Peng, R. Ye, J. A. Mann, D. Zakhidov, Y. Li, P. R. Smalley*, et al.*, "Flexible boron-doped laser-induced graphene microsupercapacitors," *ACS nano,* vol. 9, pp. 5868-5875, 2015.

[22] X. Chen, R. Paul, and L. Dai, "Carbon-based supercapacitors for efficient energy storage," *National Science Review,* vol. 4, pp. 453-489, 2017.

[23] W. Gao, N. Singh, L. Song, Z. Liu, A. L. M. Reddy, L. Ci*, et al.*, "Direct laser writing of micro-supercapacitors on hydrated graphite oxide films," *Nature Nanotechnology,* vol. 6, p. 496, 2011.

[24] M. F. El-Kady, V. Strong, S. Dubin, and R. B. Kaner, "Laser scribing of high-performance and flexible graphene-based electrochemical capacitors," *Science,* vol. 335, pp. 1326-1330, 2012.

[25] F. Wen, C. Hao, J. Xiang, L. Wang, H. Hou, Z. Su*, et al.*, "Enhanced laser scribed flexible graphene-based micro-supercapacitor performance with reduction of carbon nanotubes diameter," *Carbon,* vol. 75, pp. 236-243, 2014.

[26] M. H. Amiri, N. Namdar, A. Mashayekhi, F. Ghasemi, Z. Sanaee, and S. Mohajerzadeh, "Flexible micro supercapacitors based on laser-scribed graphene/ZnO nanocomposite," *Journal of Nanoparticle Research,* vol. 18, p. 237, 2016.

[27] J. Y. Hwang, M. F. El-Kady, Y. Wang, L. Wang, Y. Shao, K. Marsh*, et al.*, "Direct preparation and processing of graphene/RuO2 nanocomposite electrodes for high-performance capacitive energy storage," *Nano Energy,* vol. 18, pp. 57-70, 2015.

[28] H. Liu, P. He, Z. Li, Y. Liu, and J. Li, "A novel nickel-based mixed rare-earth oxide/activated carbon supercapacitor using room temperature ionic liquid electrolyte," *Electrochimica Acta,* vol. 51, pp. 1925-1931, 2006.

[29] A. Balducci, R. Dugas, P.-L. Taberna, P. Simon, D. Plee, M. Mastragostino*, et al.*, "High temperature carbon–carbon supercapacitor using ionic liquid as electrolyte," *Journal of Power Sources,* vol. 165, pp. 922-927, 2007.

[30] T. Y. Kim, H. W. Lee, M. Stoller, D. R. Dreyer, C. W. Bielawski, R. S. Ruoff*, et al.*, "High-performance supercapacitors based on poly (ionic liquid)-modified graphene electrodes," *ACS nano,* vol. 5, pp. 436-442, 2010.

[31] A. Lewandowski, A. Olejniczak, M. Galinski, and I. Stepniak, "Performance of carbon–carbon supercapacitors based on organic, aqueous and ionic liquid electrolytes," *Journal of Power Sources,* vol. 195, pp. 5814-5819, 2010.

[32] Y. Chen, X. Zhang, D. Zhang, P. Yu, and Y. Ma, "High performance supercapacitors based on reduced graphene oxide in aqueous and ionic liquid electrolytes," *Carbon,* vol. 49, pp. 573-580, 2011.

[33] W.-Y. Tsai, R. Lin, S. Murali, L. L. Zhang, J. K. McDonough, R. S. Ruoff*, et al.*, "Outstanding performance of activated graphene based supercapacitors in ionic liquid electrolyte from– 50 to 80 C," *Nano Energy,* vol. 2, pp. 403-411, 2013.

[34] Y. J. Kang, H. Chung, C.-H. Han, and W. Kim, "All-solid-state flexible supercapacitors based on papers coated with carbon nanotubes and ionic-liquid-based gel electrolytes," *Nanotechnology,* vol. 23, p. 065401, 2012.

[35] M. F. El-Kady and R. B. Kaner, "Scalable fabrication of high-power graphene micro-supercapacitors for flexible and on-chip energy storage," *Nature communications,* vol. 4, p. ncomms2446, 2013.

[36] C. Zhong, Y. Deng, W. Hu, J. Qiao, L. Zhang, and J. Zhang, "A review of electrolyte materials and compositions for electrochemical supercapacitors," *Chemical Society Reviews,* vol. 44, pp. 7484-7539, 2015.

[37] A. Brandt, S. Pohlmann, A. Varzi, A. Balducci, and S. Passerini, "Ionic liquids in supercapacitors," *MRS bulletin,* vol. 38, pp. 554-559, 2013.

[38]   D. L. Pavia, G. M. Lampman, G. S. Kriz, and J. A. Vyvyan, *Introduction to Spectroscopy*: Cengage Learning, 2014.

[39]   E. N. Kaufmann, *Characterization of Materials*: John Wiley & Sons, Incorporated, 2012.

[40]   D. Harvey, *Modern Analytical Chemistry*: McGraw-Hill, 2000.

[41]   B. E. Warren, *X-ray Diffraction*: Dover Publications, 1990.

[42]   P. W. Hawkes and J. C. H. Spence, *Science of Microscopy*: Springer New York, 2008.

[43]   Z. Peng, J. Lin, R. Ye, E. L. Samuel, and J. M. Tour, "Flexible and stackable laser-induced graphene supercapacitors," *ACS applied materials & interfaces,* vol. 7, pp. 3414-3419, 2015.

[44]   J. B. In, B. Hsia, J.-H. Yoo, S. Hyun, C. Carraro, R. Maboudian*, et al.*, "Facile fabrication of flexible all solid-state micro-supercapacitor by direct laser writing of porous carbon in polyimide," *Carbon,* vol. 83, pp. 144-151, 2015.

[45]   J. Lin, Z. Peng, Y. Liu, F. Ruiz-Zepeda, R. Ye, E. L. Samuel*, et al.*, "Laser-induced porous graphene films from commercial polymers," *Nature communications,* vol. 5, p. 5714, 2014.

[46]   Z. Qin, T. He, and Y. Zhang, "Characteristics of the conductive polyimide film surfaces induced by ultraviolet laser beam," *Applied Physics A,* vol. 66, pp. 441-443, 1998.

[47]   N. D. Luong, U. Hippi, J. T. Korhonen, A. J. Soininen, J. Ruokolainen, L.-S. Johansson*, et al.*, "Enhanced mechanical and electrical properties of polyimide film by graphene sheets via in situ polymerization," *Polymer,* vol. 52, pp. 5237-5242, 2011.

[48]   M. S. Brennesholtz and E. H. Stupp, *Projection Displays*: Wiley, 2008.

[49]   N. Mishra, S. Shinde, R. Vishwakarma, S. Kadam, M. Sharon, and M. Sharon, "MWCNTs synthesized from waste polypropylene plastics and its application in super-capacitors," in *AIP Conference Proceedings*, 2013, pp. 228-236.

[50]   S. Kannappan, K. Kaliyappan, R. K. Manian, A. S. Pandian, H. Yang, Y. S. Lee*, et al.*, "Graphene based supercapacitors with improved specific capacitance and fast charging time at high current density," *arXiv preprint arXiv:1311.1548,* 2013.

[51]   B. G. S. Raj, J. J. Wu, A. M. Asiri, and S. Anandan, "Hybrid SnO 2–Co 3 O 4 nanocubes prepared via a CoSn (OH) 6 intermediate through a sonochemical route for energy storage applications," *RSC Advances,* vol. 6, pp. 33361-33368, 2016.

[52]   S. Teng, G. Siegel, W. Wang, and A. Tiwari, "Carbonized wood for supercapacitor electrodes," *ECS Solid State Letters,* vol. 3, pp. M25-M28, 2014.